

## The circadian clock regulates autophagy directly through the nuclear hormone receptor Nr1d1/Rev-erb $\alpha$ and indirectly via Cebpb/(C/ebp $\beta$ ) in zebrafish

Guodong Huang<sup>a,b</sup>, Fanmiao Zhang<sup>a,b</sup>, Qiang Ye<sup>a,b</sup>, and Han Wang<sup>a,b</sup>

<sup>a</sup>Center for Circadian Clocks, Soochow University; Suzhou, Jiangsu, China; <sup>b</sup>School of Biology & Basic Medical Sciences, Medical College, Soochow University, Suzhou, Jiangsu, China

### ABSTRACT

Autophagy is a highly conserved intracellular degradation system, and recently was shown to display circadian rhythms in mice. The mechanisms underlying circadian regulation of autophagy, however, are still unclear. Here, we observed that numbers of autophagosomes and autolysosomes exhibit daily rhythms in the zebrafish liver, and *cebpb/(c/ebp $\beta$ )* and various autophagy genes are rhythmically expressed in zebrafish larvae but significantly upregulated in *per1b* and TALEN-generated *nr1d1/rev-erb $\alpha$*  mutant fish, indicating that both Per1b and Nr1d1 play critical roles in autophagy rhythms. Luciferase reporter and ChIP assays show that the circadian clock directly regulates autophagy genes through Nr1d1, and also regulates transcription of *cebpb* through Per1b. We also found that fasting leads to altered expression of both circadian clock genes and autophagy genes in zebrafish adult peripheral organs. Further, transcriptome analysis reveals multiple functions of Nr1d1 in zebrafish. Taken together, these findings provide evidence for how the circadian clock regulates autophagy, imply that nutritional signaling affects both circadian regulation and autophagy activities in peripheral organs, and shed light on how circadian gene mutations act through autophagy to contribute to common metabolic diseases such as obesity.

### ARTICLE HISTORY

Received 24 June 2015  
Revised 10 April 2016  
Accepted 25 April 2016

### KEYWORDS

autophagy; Cebpb/(C/ebp $\beta$ ); circadian; Nr1d1/Rev-erb $\alpha$ ; Per1b; zebrafish

### Introduction

Virtually all organisms from cyanobacteria to mammals possess the circadian clock that allows for them to anticipate environmental changes and coordinate their behavior and physiology.<sup>1,2</sup> The mammalian master clock in the suprachiasmatic nucleus (SCN) coordinates and synchronizes peripheral oscillators in most tissues and organs.<sup>3</sup> In both SCN neurons and peripheral tissues and organs, the circadian clock exerts its regulatory role through 2 highly conserved negative feedback loops. The bHLH-PAS transcriptional factors CLOCK and ARNT1/BMAL1, formed as a heterodimer, bind to the *cis* element E/E'-box (CACGT[G/T]/CANNTG) in the promoter regions of their target genes including *PER/PERIOD* and *CRY/CRYPTOCHROME* and activate their expression.<sup>4</sup> PER and CRY, formed as the other heterodimer, translocate to the nucleus and inhibit E/E'-box-mediated transcription by interacting with the CLOCK-ARNT1/BMAL1 heterodimer, fulfilling the negative feedback loop.<sup>5</sup> In addition, 2 subfamilies of nuclear hormone receptors, NR1D/Rev-erbs (NR1D1/Rev-erb $\alpha$  and NR1D2/Rev-erb $\beta$ ) and NR1F/RORs (NR1F1/RORA/ROR $\alpha$ , NR1F2/RORB/ROR $\beta$  and NR1F3/RORC/ROR $\gamma$ ), either repress or activate gene transcription through competing to bind to RORE motifs (RGGTCA/RGGTCACTRGGTCA) in the promoter regions of their


downstream genes, constituting the second feedback loop of circadian regulation.<sup>6,7</sup>

Autophagy is an evolutionarily conserved process in eukaryotes by which the cytoplasmic cargo is sequestered inside double-membrane vesicles and delivered to the lysosome for degradation.<sup>8</sup> This process not only removes misfolded proteins and damaged organelles but also is an adaptive response for providing nutrients and energy under various stresses.<sup>9</sup> The ATG1/ULK1 complex is an essential positive regulator in autophagy initiation.<sup>10,11</sup> In mice, the mechanistic target of rapamycin (serine/threonine kinase) complex 1 (MTORC1) phosphorylates the ULK1 protein and inhibits autophagy initiation when nutrients are abundant.<sup>12</sup> Genetic disruption of autophagy genes promotes tumorigenesis and accumulation of ubiquitinated protein aggregates.<sup>13</sup>

Autophagic vacuoles vary daily in rat tissues,<sup>14,15</sup> and transcription factor CEBPB has recently been found to link autophagy to the circadian clock and maintain nutrient homeostasis in mice.<sup>16</sup> The nuclear receptor NR1D1/Rev-erb $\alpha$ , highly expressed in the liver and adipose tissue, plays regulatory roles in adipogenesis, macrophage inflammatory response, and lipid, bile acid and glucose metabolism.<sup>6,17-19</sup> Heme involved in cellular redox balance and mitochondrial respiration is the endogenous ligand for NR1D1.<sup>20,21</sup> NR1D1 deficiency results in

**CONTACT** Han Wang  [han.wang88@gmail.com](mailto:han.wang88@gmail.com), [wanghan@suda.edu.cn](mailto:wanghan@suda.edu.cn)  Center for Circadian Clocks, Soochow University, 199 Renai, SIP, Suzhou 215123, Jiangsu, China.

Color versions of one or more of the figures in the article can be found online at [www.tandfonline.com/kaup](http://www.tandfonline.com/kaup).

 Supplemental data for this article can be accessed on the [publisher's website](http://www.tandfonline.com/kaup).

© 2016 Guodong Huang, Fanmiao Zhang, Qiang Ye, and Han Wang. Published with license by Taylor & Francis.

This is an Open Access article distributed under the terms of the Creative Commons Attribution-Non-Commercial License (<http://creativecommons.org/licenses/by-nc/3.0/>), which permits unrestricted non-commercial use, distribution, and reproduction in any medium, provided the original work is properly cited. The moral rights of the named author(s) have been asserted.

reduced mitochondrial content and oxidative function as well as altered autophagy activities in skeletal muscle of mice.<sup>22</sup> However, the molecular mechanisms underlying circadian regulation of autophagy rhythms are still not elucidated.

The zebrafish (*Danio rerio*) is an attractive model for studying the circadian clock and autophagy.<sup>23–25</sup> Zebrafish as a diurnal species display robust daily changes in physiology and behavior, for instance, zebrafish locomotor activities peak during the daytime but their melatonin production peaks during the nighttime, reminiscent of humans.<sup>25</sup> Using various genetic tools including TALEN (transcription activator-like effector nucleases),<sup>26–29</sup> a number of zebrafish circadian mutants have been generated for dissecting molecular genetic pathways underlying their time-keeping mechanisms.<sup>30–32</sup> Zebrafish's optical clarity of embryos, external development, and the related versatile transgenic, mutational and imaging tools have made them become important for studying vertebrate autophagy.<sup>23,33</sup> Whether zebrafish autophagy displays daily rhythms as well as possible underlying regulatory mechanisms, however, have not been investigated to date.

In this study, we found that autophagy displays robust circadian rhythms in the zebrafish liver and larvae, and autophagy genes and autophagy activities are markedly upregulated and lose rhythmicity in both TALEN-generated *nr1d1* mutant fish and viral insertional *per1b* mutant fish,<sup>30</sup> suggesting that both Nr1d1 and Per1b are critical for maintaining autophagy rhythms in zebrafish. We revealed that both E-box-mediated and RORE-mediated transcriptional regulatory mechanisms contribute to circadian regulation of autophagy rhythms. Nr1d1 is also essential for the zebrafish circadian clock, as evidenced by altered expression of core circadian clock genes and disrupted locomotor rhythms in *nr1d1* mutant fish. In addition, our transcriptome analysis reveals extensive roles of Nr1d1 in numerous life processes. These findings ascertain circadian roles in autophagy, define Nr1d1's essential functions in zebrafish circadian regulation, and provide insights into how circadian misalignment derived from mutations of circadian clock genes such as *nr1d1* likely contributes to common metabolic diseases such as obesity.

## Results

### Autophagy rhythms in zebrafish

To determine autophagy rhythmicity in zebrafish, we used transmission electron microscopy (TEM) to examine autophagosome and autolysosome numbers in the zebrafish liver at time-of-day-specific points.<sup>34</sup> We observed that numbers of autophagosomes and autolysosomes display robust oscillations, peaking at ZT 0 (Zeitgeber Time), tapering off during the day and rising again during the night, suggesting autophagosome/autolysosome rhythms in zebrafish (Fig. 1A and B). Next, we examined expression patterns of autophagy genes and autophagy-related genes in larvae through quantitative RT-PCR and JTK-CYCLE analyses.<sup>2</sup> Results show that *atg4a* (autophagy related 4A, cysteine peptidase), *atp6v1d* (ATPase, H<sup>+</sup> transporting, lysosomal V1 subunit D), *becn1/beclin1* (beclin 1, autophagy related), *ulk1a/ulk1b* (*unc-51 like autophagy activating kinase 1a/b*), *bnip3* (BCL2/adenovirus E1B interacting protein 3),

*gabarapa* (GABA(A) receptor-associated protein a), and *map1lc3b* (microtubule-associated protein 1 light chain 3  $\beta$ ), which are involved in the autophagosome initiation, nucleation, elongation, fusion, induction, substrate targeting, and degradation, are all rhythmically expressed in zebrafish larvae under LD (Light/Dark) condition with statistical significance ( $9.605 \leq F_{11,24} \leq 521.855$ , one-way ANOVA,  $P \leq 0.001$ ) (Fig. 1C and S1A), suggesting that transcription of autophagy and autophagy-related genes is regulated by the circadian clock and development in larvae.<sup>35</sup> Like autophagosomes and autolysosomes in the liver, these autophagy or autophagy-related genes peak at ZT 0, trough during the day and rise up in the night (Fig. 1C). We also analyzed the expression patterns of these autophagy genes in the adult zebrafish liver. Results show that these genes are downregulated after the morning feeding but upregulated in the night with statistical significance ( $17.501 \leq F_{11,24} \leq 351.503$ , one-way ANOVA,  $P \leq 0.001$ ) (Fig. 1D and S1B). In addition, we observed that autophagy or autophagy-related genes show 2 peaks during daytime compared with nighttime, likely due to scheduled feedings,<sup>36</sup> suggesting that the circadian clock and nutritional signals both affect their transcription in the adult zebrafish liver. We also examined expression of several core circadian clock genes including *per1b*, *nr1d1*, *clockb/clock1b* and *arntl1b/bmal1b*, and found that these 4 circadian clock genes all display rhythmic expression in zebrafish larvae on LD conditions (Fig. S1F), implicating that the circadian clock may play a role in regulating rhythmic expression of these autophagy and autophagy-related genes in zebrafish.

Map1lc3b is a zebrafish ortholog of yeast Atg8 that undergoes conjugation to phosphatidylethanolamine upon autophagy induction.<sup>24</sup> The unconjugated LC3 (LC3-I) is localized in the cytosol, whereas the lipid-conjugated form (LC3-II) resides on the phagophore and autophagosome membrane.<sup>23,37</sup> SQSTM1/p62 (sequestosome 1) is a protein that interacts with LC3 and delivers autophagy cargos for liposomal degradation.<sup>38</sup> Western blotting assays show that Map1lc3b-II displays obvious oscillations in zebrafish larvae under the LD condition, suggesting that autophagy fluxes are regulated by the circadian clock (Fig. S1C, S1D and S1E). However, Sqstm1 does not show daily changes (Fig. S1C, S1D and S1E), likely affected by developmental regulation in zebrafish.<sup>39</sup> Together, these results suggest that the autophagy activities, as evidenced by the numbers of autophagosomes and autolysosomes, the expression patterns of autophagy or autophagy-related genes and the conversion ratio of Map1lc3b-I to Map1lc3b-II, display robust daily rhythms in the zebrafish larvae and liver.

### Generation of zebrafish *nr1d1* mutants

We used an on-line TALEN design web site (<https://tale-nt.cac.cornell.edu/>) to design a pair of TALEN arms targeting the second exon of zebrafish *nr1d1*, and the targeted fragment harbors a BslI enzyme site for evaluating mutagenesis efficiency and subsequent mutant identification (Fig. 2A).<sup>40</sup> We employed the "unit assembly" method to construct the 2 *nr1d1* TALEN arms.<sup>41</sup> Capped mRNAs of these 2 TALEN arms were coinjected into one-cell stage zebrafish embryos at a concentration of 250 pg each. To evaluate the mutagenesis efficiency, a

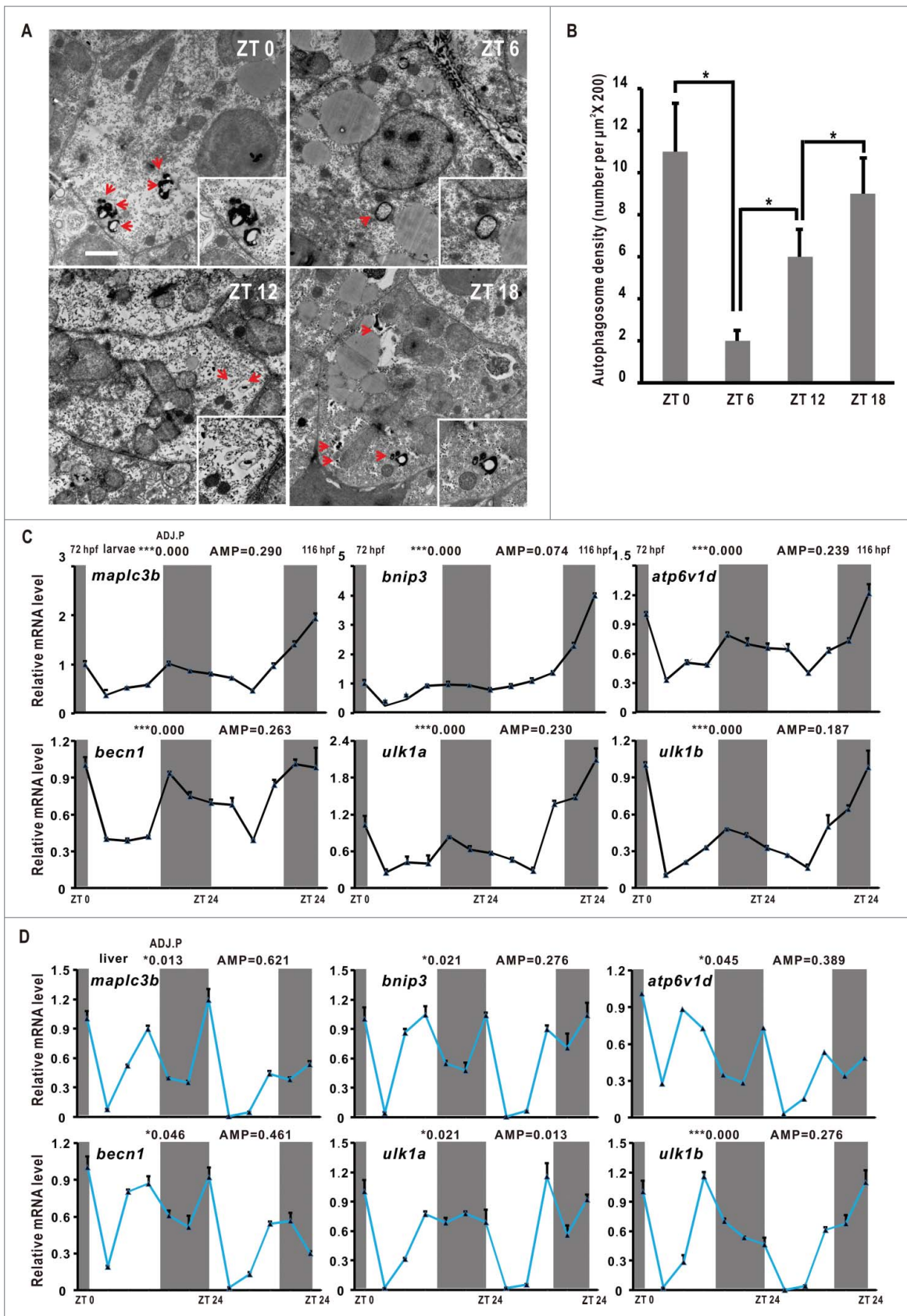


**Figure 1.** Autophagy rhythms in zebrafish. (A) Transmission electron micrograph of the zebrafish liver sections at ZT 0, ZT 6, ZT 12 and ZT 18. The scale bar in the bottom left corner of ZT 0 panel represents one micron. High magnification in the right low corners highlights a cytosolic region. Note the presence of double-membrane autophagosomes and autolysosomes (red arrowhead). (B) Quantification of autophagosome and autolysosome abundance in (A). Data represent mean  $\pm$  s.e. \*\*,  $P \leq 0.01$ . The Student  $t$  test was conducted. (C) RT-PCR analysis of expression of *map1lc3b*, *bnip3*, *atp6v1d*, *becn1*, *ulk1a* and *ulk1b* in zebrafish larvae from 72 hpf to 96 hpf. Zebrafish were maintained at 14 h light and 10 h dark condition. Approximately 50 zebrafish larvae were pooled for each time point. (D) RT-PCR analysis of expression of *map1lc3b*, *bnip3*, *atp6v1d*, *becn1*, *ulk1a* and *ulk1b* in zebrafish livers. Livers from 5 adult zebrafish were pooled for each time point. The mRNA expression levels were analyzed by the JTK-CYCLE method. ADJ.P for adjusted minimal  $P$  values (\*,  $P \leq 0.05$ ; \*\*\*,  $P \leq 0.001$ ), AMP for amplitude. One-way ANOVA was conducted (\*\*\*,  $P \leq 0.001$ ). Data represent mean  $\pm$  s.d. of the 3 independent experiments.

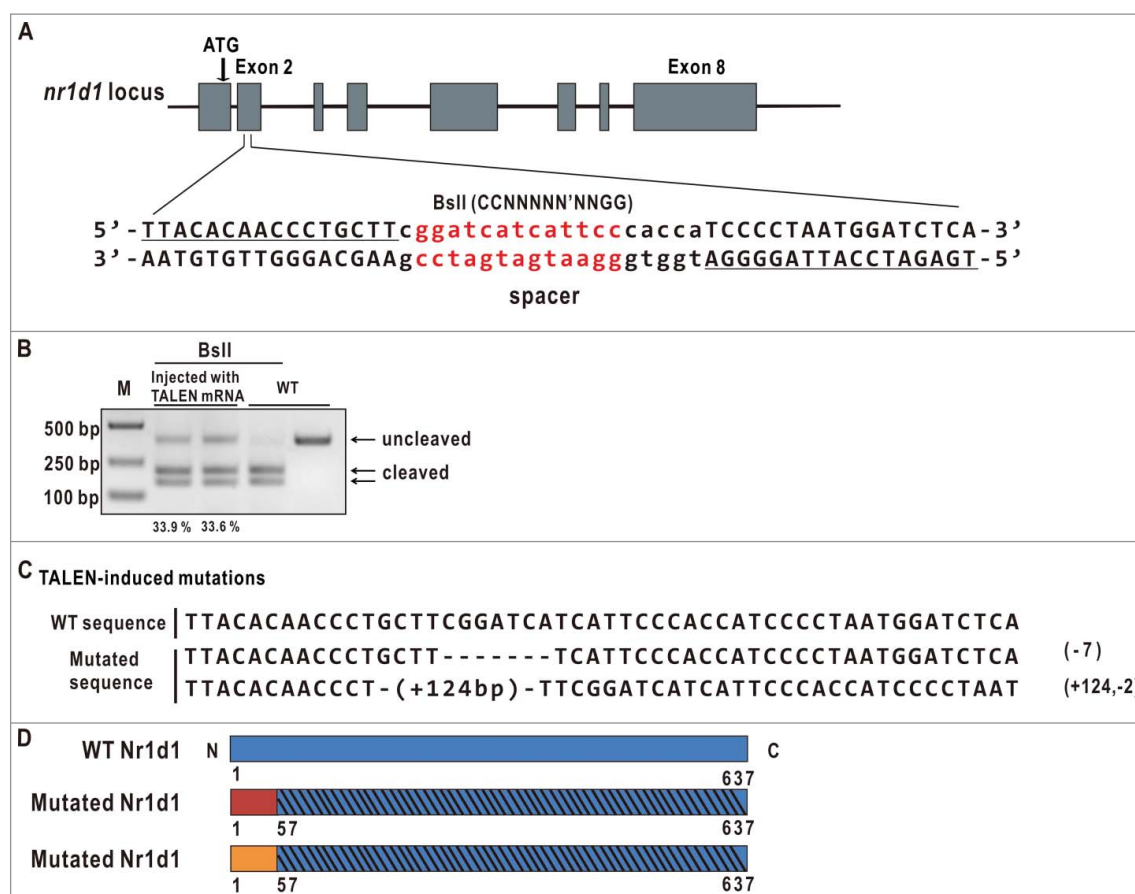


**Figure 2.** Generation of zebrafish *nr1d1* mutants. (A) Diagram of the TALEN target fragment in zebrafish *nr1d1*. The left and right TALEN arms are underlined; the TALEN spacer containing a BsalI restriction enzyme site (in red) is in small case. (B) Examine TALEN efficiencies by gel analysis. The *nr1d1* target fragment was amplified by PCR from genomic DNAs of approximately 10 embryos microinjected with capped mRNAs of *nr1d1* TALEN left and right arms at a concentration of 300 pg each, and digested with BsalI. Mutagenesis efficiencies were estimated by the ratios of the uncleaved bands and the sum of the cleaved bands and the uncleaved bands quantified with software ImageJ. WT, wild type; M, marker. (C) Two mutated fish lines were identified with DNA sequencing. One has a 7-bp deletion, the other has a 124-bp insertion and a 2-bp deletion, and both lead to frame shift mutations resulting in truncated proteins. (D) The predicted truncated Nr1d1 proteins induced by TALEN. The 2 truncated Nr1d1 proteins each have only 57 amino acids.

430-bp (base pair) fragment containing the TALEN-targeted site was PCR amplified with DNAs extracted from injected and uninjected control embryos (10 each). Enzymatic digestion of the PCR-amplified fragment with BsalI estimated approximately 33% of mutagenesis frequency (Fig. 2B). Siblings of TALEN-injected F<sub>0</sub> embryos were raised to adulthood, and then outcrossed with wild type to produce F<sub>1</sub>s. Enzymatic and DNA sequencing analyses of the targeted fragment PCR-amplified from F<sub>1</sub> fin-clipped DNAs identified 2 types of heritable mutations: one has a 7-bp deletion and the other a 122 bp (+124, -2) insertion; both induce frame shift mutations resulting in a truncated peptide of 57 AA (Fig. 2C and 2D). The homozygous mutant fish with the 7-bp deletion were used for most of the subsequent experiments.

#### Altered expression of key circadian clock genes and disrupted locomotor activities in *nr1d1* mutant zebrafish

Locomotor activities of zebrafish larvae exhibit robust circadian rhythmicity and peak during the subjective day.<sup>42</sup> We performed locomotor experiments for the *nr1d1* mutant and wild-type larvae from 5 d postfertilization (dpf) to 7 dpf. Under LD conditions, *nr1d1* larvae display significantly increased locomotor activities compared with wild type (Fig. 3A and 3B). Indeed,

the amplitude of *nr1d1* mutant larvae increases more than 40% during the whole duration of a 24-h day and night (Fig. 3E). Under the DD (dark/dark) condition, *nr1d1* larvae also display increased amplitude, though much dampened, approximately half-an-hour phase delay and 0.25-h shortened period compared with wild types (Fig. 3C, 3D and 3F). Altered behaviors of *nr1d1* mutant fish are consistent with *nr1d1* knockout mice that display mania-like behavior.<sup>43</sup>

We also examined expression patterns of core circadian clock genes in *nr1d1* mutant larvae under DD condition. Both *arntl1b/bmal1b* and *arntl2/bmal2* are significantly upregulated in *nr1d1* mutant larvae ( $1845.768 \leq F_{6,28} \leq 3435.709$ , 2-way ANOVA,  $P \leq 0.001$ ), consistent with our previous study exhibiting that Nr1d1 represses *arntl1b/bmal1b* transcription through RORE (Fig. 3I).<sup>32</sup> Moreover, *per1a* is also significantly upregulated ( $F_{6,28} = 2006.444$ , 2-way ANOVA,  $P \leq 0.001$ ), *cry1aa*, and *per1b* are significantly downregulated ( $106.233 \leq F_{6,28} \leq 206.737$ , 2-way ANOVA,  $P \leq 0.001$ ), and *cry1ab*, *per2*, and *per3* are phase-delayed ( $146.821 \leq F_{6,28} \leq 1619.126$ , 2-way ANOVA,  $P \leq 0.001$ ), in *nr1d1* mutant larvae (Fig. 3I), even though they still maintain rhythmicity (Fig. 3I). Together, these results suggest that Nr1d1 plays an essential role in regulating circadian clock genes and behavior in zebrafish.

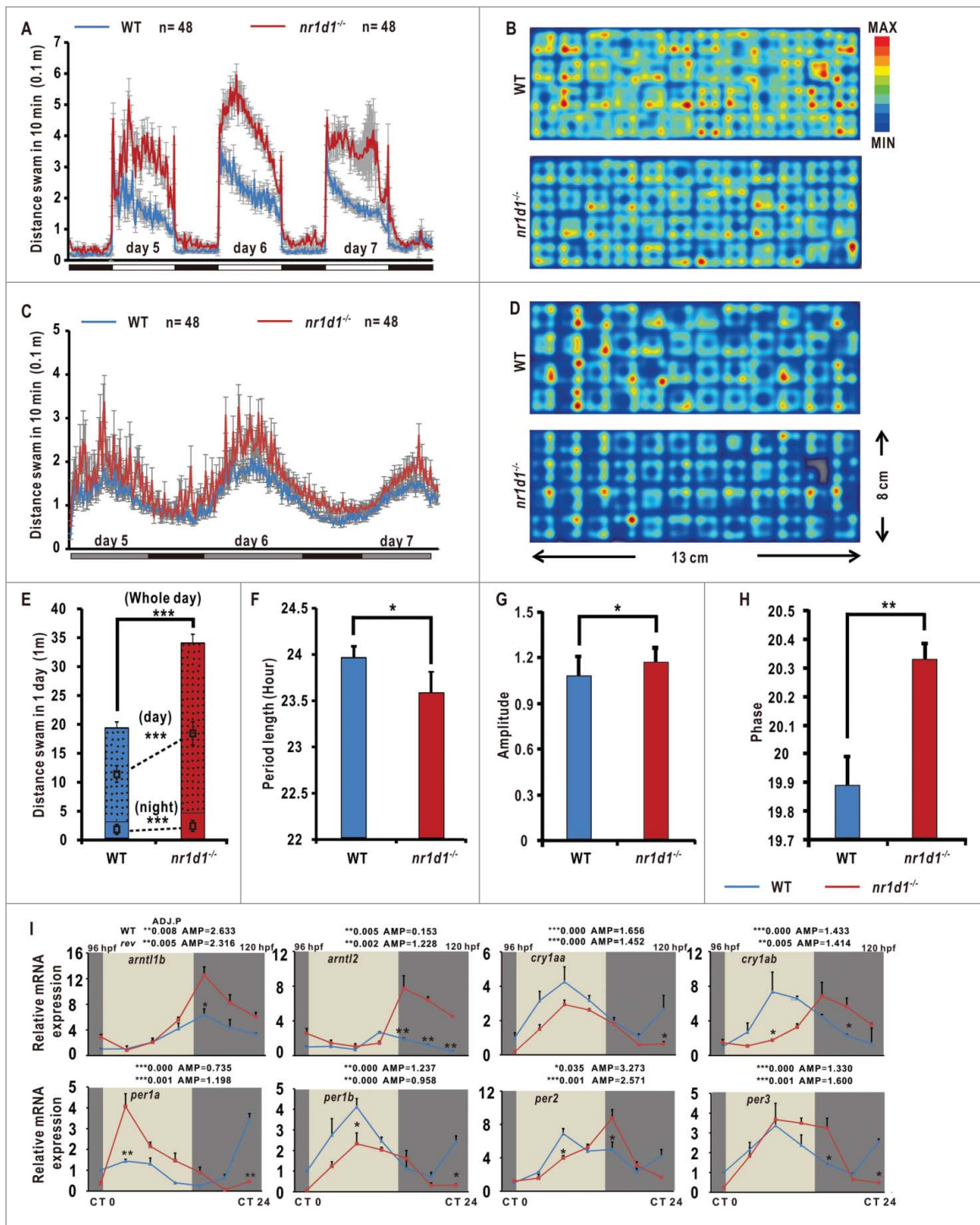


**Figure 3.** Disrupted rhythms of locomotor activities and altered expression of key circadian clock genes in homozygous *nr1d1* mutant zebrafish. (A, C) The locomotor assays of *nr1d1* mutant and wild-type larvae from 4 dpf to 7 dpf under LD (A) and DD (C) conditions. *nr1d1* mutants, n = 48; wild types, n = 48. (B, D) Heat maps represent the total swimming or resting area of a wild-type or *nr1d1* mutant larva in each well under LD (B) and DD (D). The spatial bin size is 10X10 mm (see scale on the right). The red colors represent more resting activities of the larvae, and the blue color more locomotor activities of the larvae. *nr1d1* mutant larvae (bottom) swim more of the perimeter in the well compared with wild types (top). (E) The average swimming distances of single wild-type and *nr1d1* larvae during one day. The upper dot box indicates the swimming distance of single larva in the day, and the bottom box the swimming distance of single larva in the night. Data represent mean ± s.d. (\*\*\*,  $P \leq 0.001$ ). (F) Histogram of the average period of wild-type and *nr1d1* larvae. Data represent mean ± s.d. (\*,  $P \leq 0.05$ ). (G) Histogram of the average swimming distances of wild-type and *nr1d1* larvae during the 3 d. Data represent mean ± s.d. (\*,  $P \leq 0.05$ ). (H) Histogram of the average phase during the 3 d. Data represent mean ± s.d. (\*\*,  $P \leq 0.01$ ). (I) Altered expression of key circadian clock genes *arntl1b*, *arntl2*, *cry1aa*, *cry1ab*, *per1a*, *per1b*, *per2*, and *per3* in *nr1d1* mutant fish under DD condition shown by qRT-PCR analyses. The mRNA expression levels were analyzed by the JTK-CYCLE method. ADJ.P for adjusted minimal  $P$ -values (\*\*\*,  $P \leq 0.001$ ), AMP for amplitude. Two-way ANOVA with the Tukey *post hoc* test was conducted (\*\*\*,  $P \leq 0.001$ ). Approximately 50 zebrafish larvae were pooled for each time point. Data represent mean ± s.d. of the 3 independent experiments.

### Loss of rhythmic expression of *cebpb*, autophagy genes and autophagy-related genes in *nr1d1* and *per1b* mutant fish

We used an mCherry-*map1lc3b* vector to monitor the acidic autolysosomes in *nr1d1* mutants.<sup>44</sup> Results show that the numbers of autolysosomes are higher in *nr1d1* mutants than in the

wild-type control (Fig. 4A and 4C). Transmission electron microscopy analysis of the adult zebrafish livers shows the increased numbers of autophagosomes and autolysosomes in *nr1d1* mutants at ZT 0 (Fig. 4B and 4D). Thus, it appears that Nr1d1 plays an essential role in autophagy activities in zebrafish.

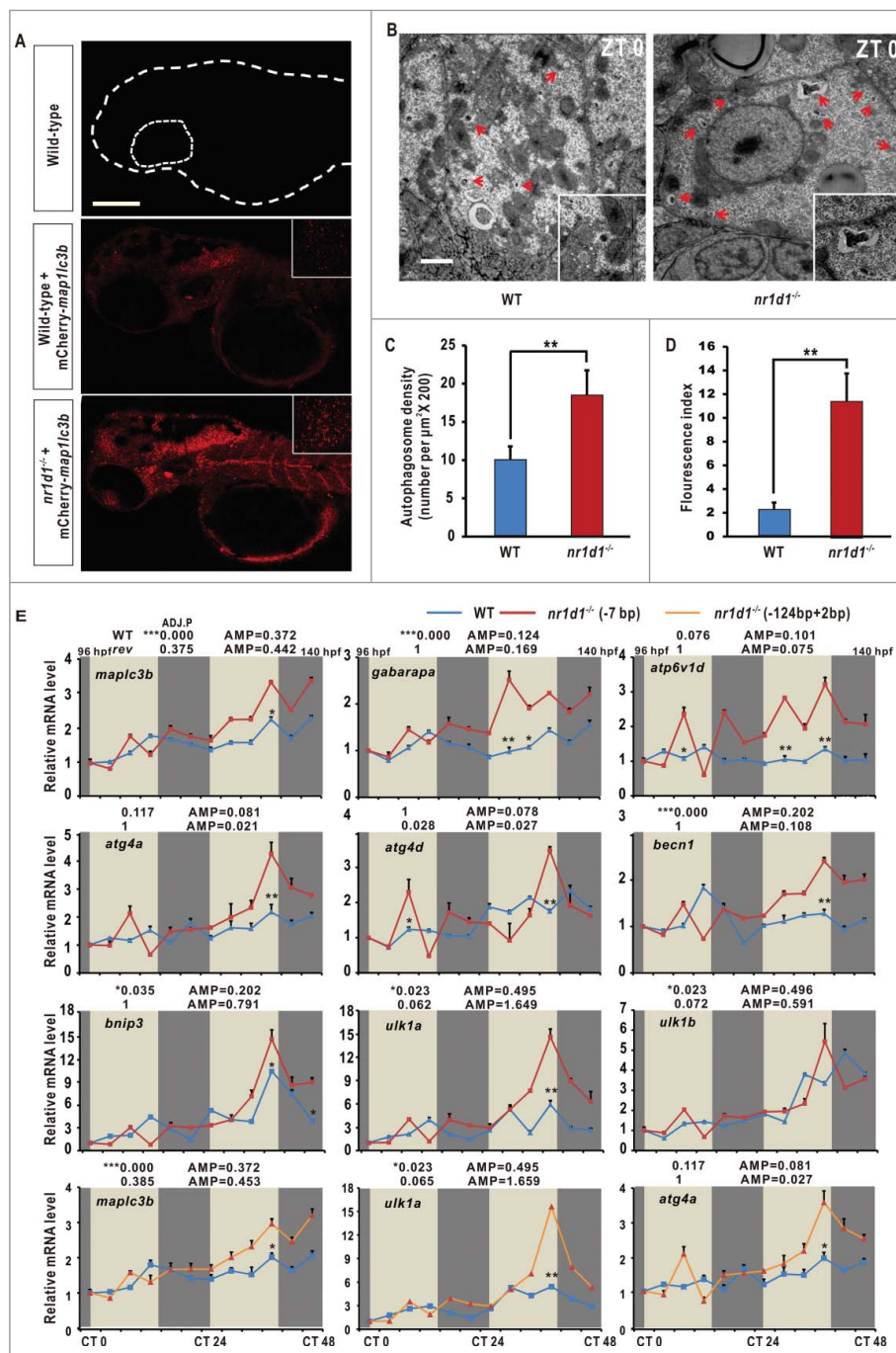


**Figure 4.** Disrupted autophagy activities and altered expression of autophagy genes in *nr1d1* mutant zebrafish. (A) Zebrafish larval autolysosomes were estimated by expression of mCherry-Map1lc3b at 56 hpf. The scale bar in the lower left of the wild-type panel represents 100 microns. The right upper panels show high magnification highlighting a hindbrain region in both wild-type and *nr1d1* mutant larva labeled with mCherry-Map1lc3b. (B) Transmission electron micrograph of wild-type and *nr1d1* mutant liver sections at ZT 0. The scale bar in the lower left of the wild-type panel represents one micron. (C) Quantification of autolysosomes in (A), calculated manually. (D) Quantification of autophagosome abundance in (B) with software ImageJ. The figure represents one of the 3 independent sets of samples. Data represent mean  $\pm$  s.d. (\*,  $P \leq 0.05$ ; \*\*,  $P \leq 0.01$ ). The Student *t* test was conducted, (\*,  $P \leq 0.05$ ; \*\*,  $P \leq 0.01$ ). (E) RT-PCR analysis of autophagy genes in *nr1d1* (-7bp or +124,-2bp) mutant zebrafish at different time points under DD condition. Zebrafish larvae were raised under light/dark (14 h/10 h) condition for the first 3 dpf, and then placed under constant darkness condition. Approximately 50 zebrafish larvae were pooled for each time point. The mRNA expression levels were analyzed by the JTK-CYCLE method. ADJ.P for adjusted minimal *p*-values (\*,  $P \leq 0.05$ ; \*\*\*,  $P \leq 0.001$ ), AMP for amplitude. Two-way ANOVA with the Tukey *post hoc* test was conducted (\*,  $P \leq 0.05$ ; \*\*,  $P \leq 0.01$ ).

Rhythmic expression of autophagy genes suggests that transcriptional regulation plays an important role in driving cyclic autophagy. The molecular components of autophagy have been extensively investigated,<sup>37,45</sup> and previous studies show that clock-controlled transcription factors CEBPB and FOXO3 play important roles in regulating transcription of autophagy genes in mice.<sup>16,46</sup> However, how the circadian clock regulates *cebpb* and whether the circadian clock directly regulates autophagy genes are still not clear. To underscore circadian regulation, we examined expression of autophagy and autophagy-related genes in *nr1d1* mutant and wild-type larvae under DD condition.<sup>35,47,48</sup> Here, qRT-PCR analyses show that *map1lc3b* and *gabapara* are significantly upregulated in *nr1d1* mutants ( $0.964 \leq F_{11,48} \leq 58.517$ , 2-way ANOVA,  $P \leq 0.001$ ) (Fig. 4E). Meanwhile, significantly upregulated *atp6v1d* mRNA level ( $F_{11,48} = 138.475$ , 2-way ANOVA,  $P \leq 0.001$ ) suggests that more autophagosomes fuse with lysosomes, forming autolysosomes in *nr1d1* mutants (Fig. 4E). Likewise, other autophagy genes or autophagy-related genes including *atg4a*, *atg4d*, *becn1*, and *bnip3* are also significantly upregulated ( $38.545 \leq F_{11,48} \leq 162.689$ , 2-way ANOVA,  $P \leq 0.001$ ); in particular, JTK-CYCLE analysis showed all these genes lose rhythmicity in *nr1d1* mutants compared with the wild-type zebrafish (Fig. 4E). As a second internal nonrhythmic gene, *tuba1b* (*tubulin*,  $\alpha 1b$ ) expression is not rhythmic in wild-type and *nr1d1* mutant larvae (ADJ.P ( $P > 0.05$ ), WT = 1.356, *nr1d1* = 1.384), and has no significant changes between wild-type and *nr1d1* mutant larvae ( $P = 0.972$ ) (Fig. S3D). Moreover, similar to what observed in the *nr1d1* (-7bp) mutant line, *map1lc3b*, *ulk1a* and *atg4a* are also significantly upregulated in the other *nr1d1* (+124, -2 bp) mutant line ( $35.367 \leq F_{11,48} \leq 141.612$ , 2-way ANOVA,  $P \leq 0.001$ ) (Fig. 4E), further corroborating that altered expression of these autophagy genes and autophagy-related genes is resulted from loss of Nr1d1 function.

qRT-PCR and JTK-CYCLE analyses also show that *cebpb* is rhythmically expressed in zebrafish with statistical significance ( $F_{11,48} = 153.434$ , 2-way ANOVA,  $P \leq 0.001$ ) (Fig. 5A), and its expression of autophagy genes and autophagy-related genes *map1lc3b*, *gabapara*, *atp6v1d*, *atg4a*, *atg4d*, *becn1*, *bnip3*, *ulk1a* and *ulk1b* are all significantly upregulated without rhythmicity in *per1b* mutant zebrafish ( $36.824 \leq F_{11,48} \leq 570.718$ , 2-way ANOVA,  $P \leq 0.001$ ) (Fig. 5A),<sup>30</sup> suggesting that *Per1b* also plays a regulatory role in expression of *cebpb*, autophagy genes and autophagy-related genes.

### Regulation of *cebpb*, autophagy genes and autophagy-related genes by the circadian clock

We observed that the zebrafish *cebpb* promoter region harbors several E-boxes and E'-boxes (Fig. 5C). Luciferase reporter assays show that activities of the zebrafish *cebpb* promoter are enhanced by *Clocka/Clock1a* and *Arntl1b/Bmal1b* but repressed by *Cry1ab* (Fig. 5B). ChIP assays show that *Arntl1b/Bmal1b* binds to the second E'-box in the zebrafish *cebpb* promoter region (Fig. 5D). Together, these results indicate that *cebpb* is regulated directly by the circadian clock via E'-box in zebrafish. Thus, it is likely that the circadian clock regulates autophagy rhythms via direct control of transcription factor *cebpb* that in turn regulates autophagy genes and autophagy-related genes.<sup>16</sup>

We also observed motifs including E-box, RORE, RevDR2, CCAAT (*cebpb* binding) motif in approximately 2, 500-bp promoter regions of these autophagy and autophagy-related genes in zebrafish,<sup>7,49,50</sup> suggesting transcription of these autophagy genes and autophagy-related genes may be regulated directly by the circadian clock components (Fig. S2).

Altered patterns of *ulk1a* and *ulk1b* in *nr1d1* or *per1b* mutants led us to hypothesize that *ulk1* transcription might be regulated directly by the circadian clock. As shown by luciferase assays, while *Clocka/Clock1a* and *Arntl1b/Bmal1b* have no effects on *ulk1a* promoter activities (Fig. S6F), *Nr1d1* or *Rora* can repress or activate *ulk1a* in a dosage-dependent manner (Fig. 6C). We observed 2 canonical RORE motifs in the *ulk1a* promoter (Fig. 6A). Luciferase assays show that deleting either RORE1 or RORE2 or both significantly reduces the *ulk1a* promoter activities, indicating that *ulk1a* is regulated directly by *Nr1d1* through RORE in vitro (Fig. 6C). To further investigate the possible role of Rev-DR2, we generated a construct wherein the Rev-DR2 motif and the 2 RORE motifs were all deleted. Results show that *ulk1a* promoter activities are significantly reduced but still not completely abolished compared with both RORE site deleted *ulk1a* promoter (Fig. 6C), suggesting that an unknown motif or motifs play certain regulatory roles in *ulk1a* transcription. ChIP assays show that *Nr1d1* binds directly to the RORE sites in the *ulk1a* promoter in vivo (Fig. 6B), indicating that *Nr1d1* directly regulates *ulk1a* in zebrafish. In addition, we also found that another autophagy-related gene *atp6v1d* is a direct target of *Nr1d1*, as evidenced by luciferase reporter and ChIP assays (Fig. S3B and S3C). Together, these results demonstrate that *Nr1d1* directly regulates autophagy genes and autophagy-related genes in zebrafish.

### Pharmacological activation of *Nr1d1* functions in zebrafish

A previous study showed that GSK4112, a *Nr1d1* agonist, can increase the repressive efficiency of *Nr1d1* through competing with the ligand heme.<sup>51</sup> We treated zebrafish larvae with 20  $\mu$ M GSK4112 and observed that *arntl1a/bmal1a* and *arntl1b/bmal1b* are both downregulated in GSK4112-treated fish, indicating that GSK4112 can enhance the repressive efficiency of *Nr1d1* in zebrafish larvae (Fig. S6A). Moreover, to evaluate effects of pharmacological treatment on expression of autophagy or autophagy-related genes, we performed qRT-PCR experiment and found that autophagy genes *ulk1a*, *ulk1b*, and *atg4d*, and autophagy-related genes *bnip3* and *atp6v1d* are all downregulated in GSK4112-treated fish (Fig. S6B). In addition, injecting capped *nr1d1* mRNAs could rescue expression of these autophagy genes in *nr1d1* mutants (Fig. S6B). We also examined protein levels of autophagy markers, *Map1lc3b* and *Sqstm1*, in *nr1d1* mutant and pharmacologically treated wild-type zebrafish larvae at different time points. Results show that *Map1lc3b* and *Sqstm1* are significantly upregulated in *nr1d1* mutants but no significant changes of *Map1lc3b* and *Sqstm1* in GSK4112-treated wild-type fish (Fig. S6C, 6D and 6E), even though *Map1lc3b* and *Sqstm1* are antiphasic in zebrafish larvae (Fig. S1C, D and E). Thus, GSK4112 treatment can affect transcription but not translation of autophagy and autophagy genes in zebrafish. These results further support that rhythmic expression of autophagy genes are under control of *Nr1d1* in zebrafish.

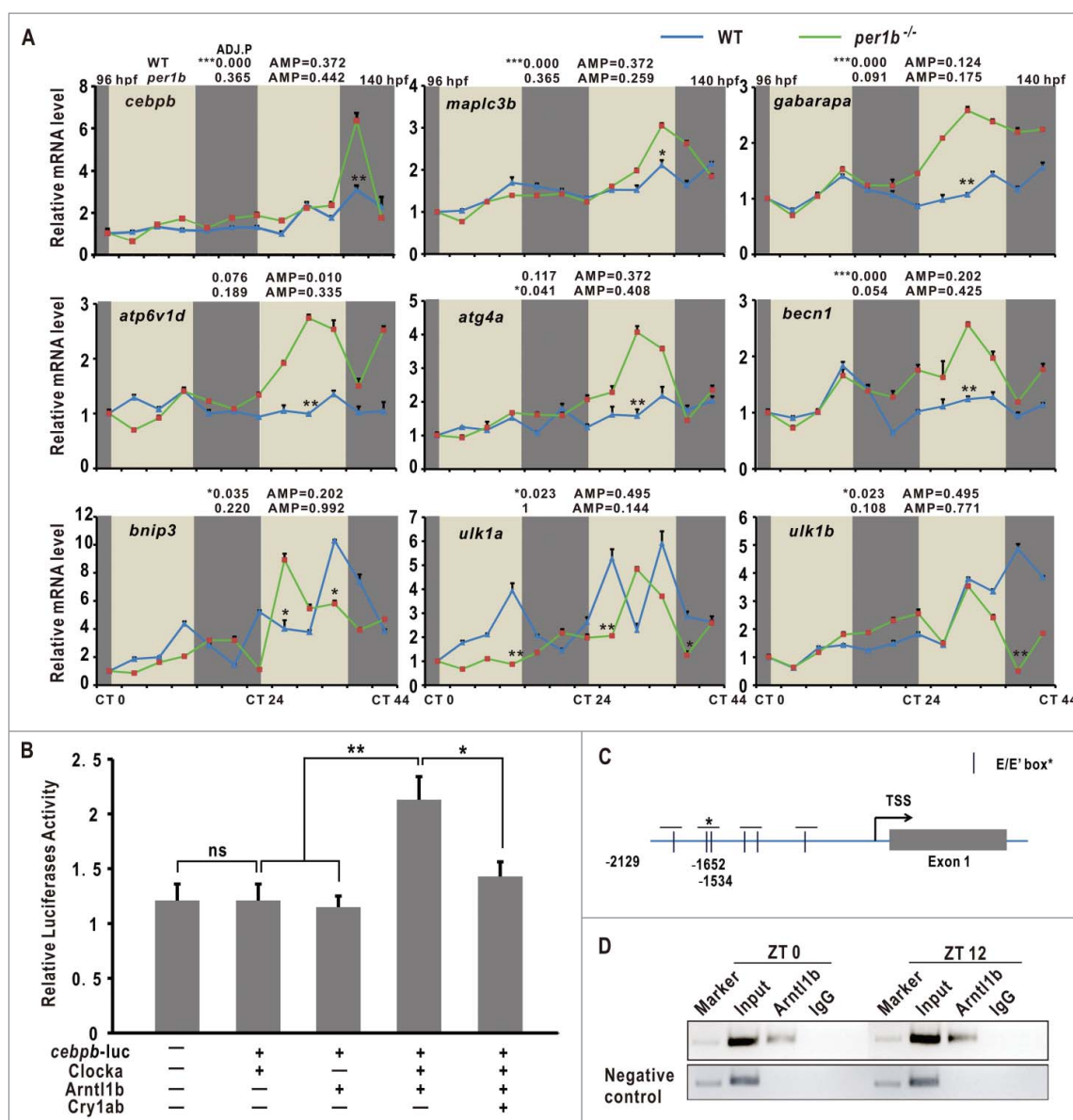


**Figure 5.** Upregulation of autophagy genes in *per1b* mutants and *cebpb* is controlled by the circadian clock in zebrafish. (A) Upregulation of autophagy genes in zebrafish *per1b* mutant larvae under DD, shown by qRT-PCR analysis. The mRNA expression levels were analyzed by the JTK-CYCLE method. ADJ.P for adjusted minimal p-values (\*,  $P \leq 0.05$ ; \*\*\*,  $P \leq 0.001$ ), AMP for amplitude. Two-way ANOVA with the Tukey *post hoc* test was conducted (\*,  $P \leq 0.05$ ; \*\*,  $P \leq 0.01$ ). (B) Luciferase reporter assays. Activities of the *cebpb* promoter are enhanced by cotransfection with *Clock1a/Clock1a* and *arntl1b* but repressed by *Cry1ab*. The *cebpb*-pGL4, *Clock1a/Clock1a*-pcDNA3.1, *Arntl1b/Bmal1b*-pcDNA3.1 and *Cry1ab*-pcDNA3.1 plasmids were transfected at the concentration of 100 ng/ $\mu$ l each. Data represent mean  $\pm$  s.d. (\*\*,  $P \leq 0.01$ ). The Student *t* test was applied. (C) Diagram of the *cebpb* promoter containing multiple E-boxes and E'-boxes. (D) ChIP assays. *Arntl1b/Bmal1b* binds to the E-boxes in the *cebpb* promoter.

### Effects of fasting and loss of *Nr1d1* on expression of circadian clock genes, and autophagy and autophagy-related genes in peripheral organs

Previous studies showed that *nr1d1* is expressed extensively in zebrafish tissues/organs and nutritional signals can affect zebrafish circadian behavior.<sup>35,52,53</sup> However, whether nutritional signaling or loss of *Nr1d1* affects the circadian clock or autophagy in peripheral organs has not yet been investigated in zebrafish. We first examined expression patterns of core circadian genes in the liver of fed *nr1d1* mutants, fasted *nr1d1* mutants, fed wild-type and fasted wild-type fish. Results show that *arntl1b/bmal1b*, *clocka/clock1a*, *cry1ab* and *per1b* are all significantly upregulated in the *nr1d1* mutant group in comparison with the wild-type control ( $57.125 \leq F_{11,48} \leq 4270.745$ ,

2-way ANOVA,  $P \leq 0.001$ ); and expression of both *clocka/clock1a* is significantly higher in fasted wild types than the fed wild-type control ( $F_{11,48} = 224.366$ , 2-way ANOVA,  $P \leq 0.001$ ), and even higher in fasted *nr1d1* mutant group than the fed *nr1d1* mutant group ( $F_{11,48} = 157.281$ , 2-way ANOVA,  $P \leq 0.001$ ) (Fig. 7A); suggesting that both nutritional signals and *nr1d1* contribute to the zebrafish liver clock.

We then examined several key autophagy and autophagy-related genes in the brain, the liver, the heart, the eye and the intestine of fed *nr1d1* mutant, fasted *nr1d1* mutant, fed wild-type and fasted wild-type fish (Fig. 7B and Fig. S3A). Consistent with what observed in the wild-type liver, these autophagy or autophagy-related genes still display 2 peaks in one day's cycling in the zebrafish heart, eye, brain and intestinal organs, suggesting synergistic regulation of their transcription by the





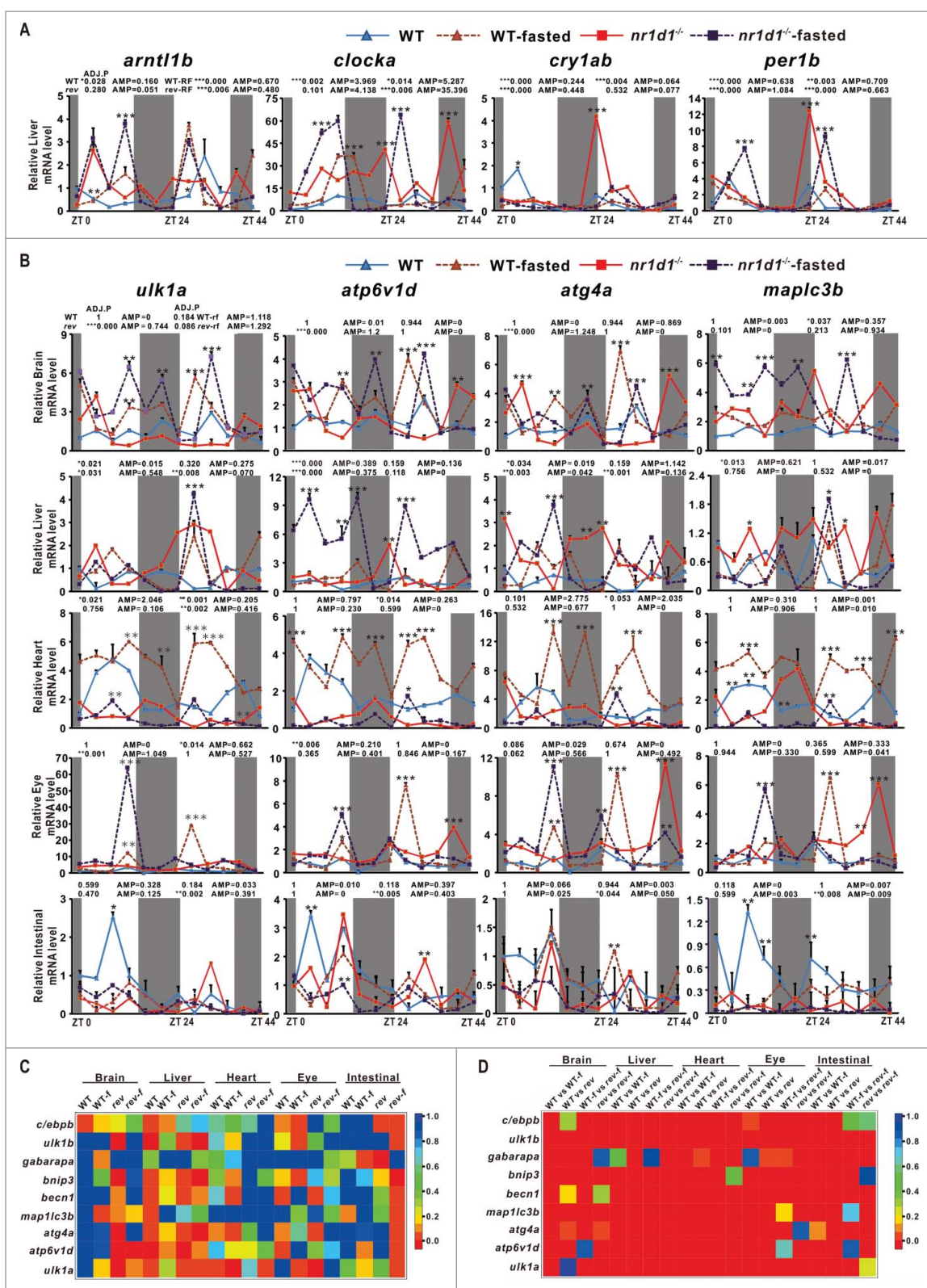


**Figure 7.** Effects of fasting and loss of Nr1d1 on expression of autophagy genes and circadian clock genes. (A) qRT-PCR analysis of core circadian clock genes in the liver of *nr1d1* mutant (fed), fasted *nr1d1* mutant, wild-type (fed) and fasted wild-type fish. (B) qRT-PCR analysis of autophagy genes *map1c3b*, *atp6v1d*, *ulk1a* and *atg4a* in the adult peripheral organs of *nr1d1* mutant, fasted *nr1d1* mutant, fasted wild-type and fasted wild-type fish under LD. Following 2-wk fasting, 4-mo-old wild-type and *nr1d1* mutant fish, and their controls were sacrificed, and the brains, the livers, the hearts, the eyes, and the intestines were dissected out and collected for RNA extraction at 12 time points with 4-h interval under LD for a total of consecutive 2 d. Each sample contains organs from at least 5 male fishes. Three independent sets of samples were used. The mRNA expression pattern was analyzed by JTK-CYCLE method. ADJ.P for adjusted minimal *P* values ( $^*$ ,  $P \leq 0.05$ ;  $^{**}$ ,  $P \leq 0.01$ ;  $^{***}$ ,  $P \leq 0.001$ ), AMP for amplitude. Two-way ANOVA with the Tukey *post hoc* test was conducted ( $^*$ ,  $P \leq 0.05$ ;  $^{**}$ ,  $P \leq 0.01$ ;  $^{***}$ ,  $P \leq 0.001$ ). (C) Heatmap comparing ADJ.P values of autophagy and autophagy-related genes in different zebrafish organs of wild-type (fed), wild-type-fasted, *nr1d1* (fed) and *nr1d1*-fasted groups. (D) Heatmap showing correlation coefficients (*R*) of *P* values from 2-way ANOVA of autophagy and autophagy-related genes in different zebrafish organs in terms of wild-type (fed) vs wild-type-fasted, wild-type (fed) vs *nr1d1* (fed), wild-type-fasted vs *nr1d1*-fasted, and *nr1d1* (fed) vs *nr1d1*-fasted. WT-f, WT-fasted.

and circadian clock genes display distinct rhythmic expression patterns in different organs, which are all significantly disrupted in fasted wild-type, fasted *nr1d1* mutant and fed *nr1d1* mutant fishes (Fig. 7A–D and Fig. S3A).

### ***Nr1d1* also contributes to stress response, metabolism, signal transduction and post-translational modification**

To examine possible effects of *Nr1d1* on other life processes, we conducted transcriptome sequencing (RNA-seq) analysis of *nr1d1* mutant and wild-type fish, and uncovered 975 differentially expressed genes (DEGs) at CT2 and 1, 360 DEGs at CT14 ( $2 \leq P \leq 5$ ) (Fig. 8A). Clustering analysis shows more upregulated genes than downregulated genes in *nr1d1* mutant fish at the indicated time points (Fig. 8B), likely because *Nr1d1* acts as a transcription repressor in zebrafish.<sup>32</sup> Through gene Ontology (GO) classification, we found that DEGs are enriched for the binding, catalytic activity in molecular functions, and metabolic process, biological regulation, developmental process, immune system and rhythmic process in biological processes (Figs. S4A and S5A). For the Kyoto Encyclopedia of Genes and Genomes (KEGG) analysis, we found that the MAPK signaling pathway shows the highest numbers of DEGs (13 at CT2 and 29 at CT12). While at CT2, we found a large number of DEGs involved in metabolism pathways like purine, pyrimidine, steroid and cytochrome P450; at CT12, DEGs trend to distribute in ribosome processing, the calcium signaling pathway, the insulin signaling pathway and oxidative phosphorylation (Figs. S4B and S5B). Further, we reconfirmed transcriptome analysis results by qRT-PCR and found upregulation of *atg10* (autophagy), *ucp3* (brown adipose tissue metabolism), *rbp4* (adipose tissue metabolism), *slc5a1* and *wdr3* (signal transduction), *exosc3* (RNA processing), *gbgt114* (immune response), *gria3a* (neurotransmission) and *ddx46* (posttranslational modification); and downregulation of *urod* (heme biosynthesis), *fn1b* (cell function) and *gsk3b* (energy metabolism) in *nr1d1* mutants (Fig. 8C and 8D). In addition, we performed the JC-1 staining experiment,<sup>54</sup> and found that the ratio of Red/Green is significantly decreased in *nr1d1* mutants, implying the low mitochondrial content in *nr1d1* mutants (Fig. 8E and F). We also observed that *ppargc1a* is significantly downregulated in *nr1d1* mutants ( $F_{11,48} = 244.142$ , 2-way ANOVA,  $P \leq 0.001$ ) (Fig. 8G). Together, our transcriptome and qRT-PCR analyses suggest that *Nr1d1* also contributes to numerous life processes including stress response, metabolism, signal transduction and post-translational modification in zebrafish.

## **Discussion**

In this study, we demonstrate that zebrafish autophagy activities including autophagosome and autolysosome numbers, expression of autophagy or autophagy-related genes and Map11c3b protein all display robust daily rhythms in the larvae and liver (Fig. 1 and S1). We employed TALEN, a versatile genome-editing tool, to generate mutant lines for nuclear hormone receptor gene *nr1d1* (Fig. 2). We found that autophagy activities including autophagosome and autolysosome numbers, expression of autophagy or autophagy-related genes and Map11c3b protein are all upregulated in *nr1d1* mutant zebrafish

(Fig. 4A and S6C), suggesting that *Nr1d1* plays a role in regulating zebrafish autophagy rhythms. Consistent with a previous mouse study,<sup>16</sup> we also show that transcription factor *cebpb* is rhythmically expressed in zebrafish but its expression and expression of autophagy or autophagy-related genes are all upregulated in a circadian mutant *per1b*,<sup>30</sup> suggesting that *Perb1* also acts to regulate zebrafish autophagy rhythms.

### **The circadian clock modulates autophagy rhythms in zebrafish**

We found that the circadian clock exerts its regulatory role in autophagy rhythms in 2 ways: one is that the Clock-Arntl/ Bmal heterodimer binds to the E-Boxes to regulate transcription of *cebpb* that in turn controls transcription of autophagy and autophagy-related genes, the other is that *Nr1d1* and *Rora* binds to the RORE motifs to directly regulate transcription of autophagy and autophagy-related genes (Fig. 8F).

To support this notion, we found several *Cebpb*-binding motifs in promoter regions of a number of autophagy or autophagy-related genes (Fig. S2), and luciferase reporter and ChIP assays indicate that *cebpb* is a circadian clock-controlled gene in zebrafish (Fig. 5B and 5D), providing clear evidence for how the circadian clock regulates *cebpb*.<sup>16</sup> We also observed RORE motifs in promoter regions of a number of autophagy and autophagy-related genes (Fig. S2). In particular, luciferase reporter assays show that *ulk1a* is activated by *Rora* but repressed by *Nr1d1* via competing to bind to 2 RORE motifs in the *ulk1a* promoter in vitro (Fig. 6C); ChIP assays show that *Nr1d1* binds to 2 RORE motifs in the *ulk1a* and *atp6v1d* promoters in vivo (Fig. 6B Fig. S3B and S3C); thus indicating a direct role of *Nr1d1* in regulation autophagy rhythms. Further evidence shows that *Nr1d1* acts to regulate rhythmic expression of autophagy and autophagy-related genes in zebrafish peripheral organs such as the liver, the brain and the heart in a tissue and organ-specific manner (Fig. 7A). We found that most autophagy and autophagy-related genes are upregulated and maintain rhythmicity in the brain of the *nr1d1* mutant (Fig. 7B, 7D and Fig. S3A). However, *cebpb* is barely altered, implicating that upregulation of autophagy activities might be resulted from loss of *Nr1d1* rather than *Cebpb* (Fig. 7B, 7D and Fig. S3A). For the heart, fasting, rather than loss of *Nr1d1*, significantly upregulates expression of autophagy and autophagy genes (Fig. 7B, 7D and Fig. S3A). Unsurprisingly, nutritional signaling affects both the zebrafish circadian clock and autophagy rhythms in the liver and *cebpb* is also upregulated in the *nr1d1* mutant (Fig. 7B, 7D and Fig. S3A), indicating that the zebrafish liver and the mouse liver display similar autophagy regulatory mechanisms via the circadian clock and *Cebpb*.<sup>16,46</sup> Intriguingly, most of these autophagy and autophagy-related genes maintain strong rhythmicity in the liver regardless of nutritional stress and circadian dysregulation (Fig. 7C), implicating that autophagy rhythms are robust in the zebrafish liver. In contrast, most of these autophagy and autophagy-related genes lose their rhythmicity in the eye and heart in *nr1d1*-fed and *nr1d1*-fasted groups (Fig. 7C), suggesting that both the circadian clock and normal nutritional status are required for cycling autophagy activities. Even though how the E-Box-mediated and RORE-mediated transcription processes may

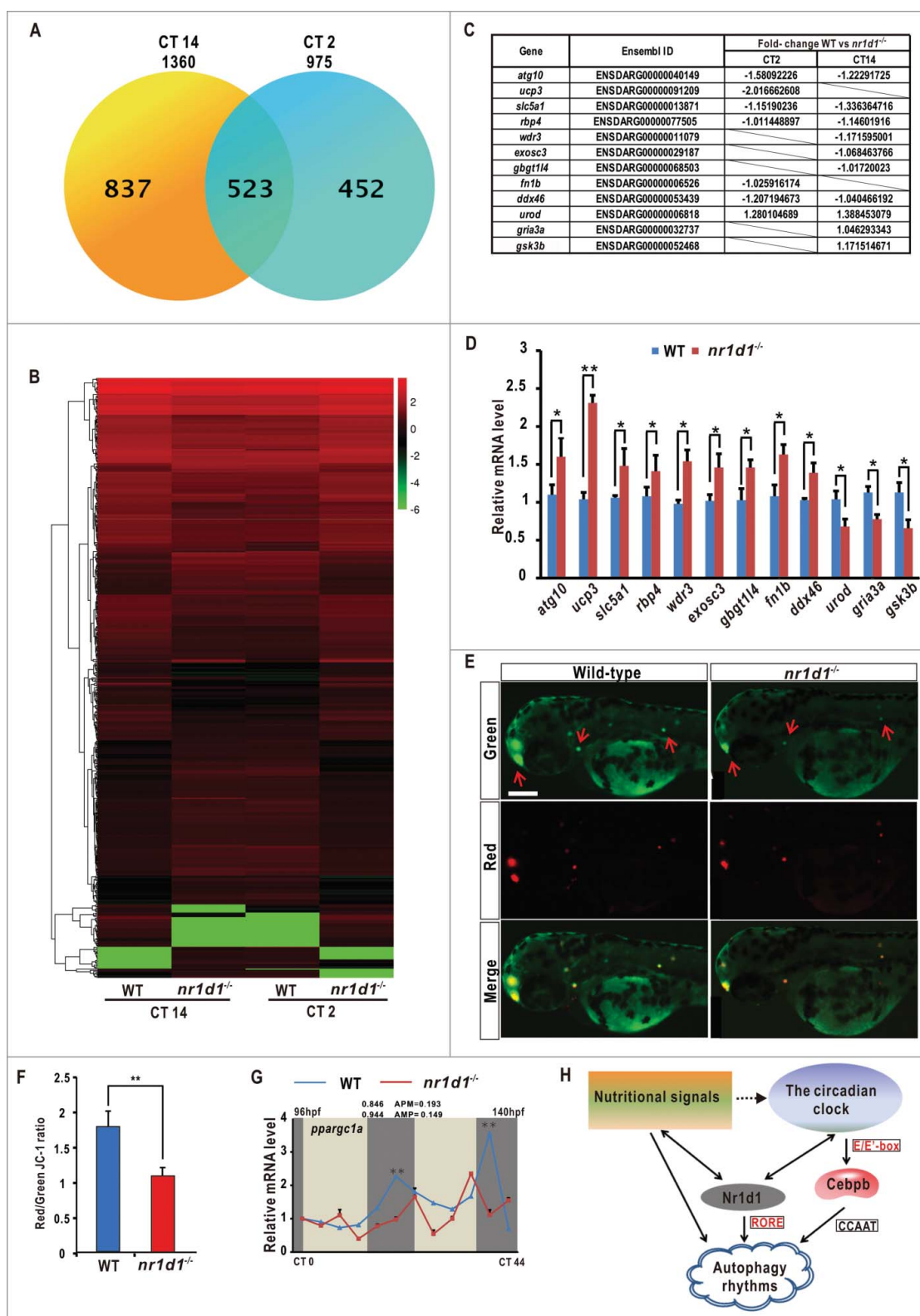


**Figure 8.** Transcriptome analysis and a model for circadian regulation of autophagy. (A) Numbers of differentially expressed genes (DEGs) in *nr1d1* mutant fish at CT2 and CT14, revealed by transcriptome analysis. (B) Histogram of 523 DEGs in *nr1d1* mutant fish shared between CT12 and CT2. Red colors represent upregulation, green colors downregulation. (C) List of genes with significant fold-changes, revealed by transcriptome analysis. The fold-changes were calculated by values of WT vs. *nr1d1/rev-erba*. Genes with positive values were downregulated in the *nr1d1* mutant, and those with negative values upregulated. (D) Upregulated genes *atg10*, *ucp3*, *slc5a1*, *rbp4*, *wdr3*, *exosc3*, *gbgt114*, *fn1b* and *ddx46* and downregulated genes *urod*, *gria3a* and *gsk3b*, revealed by transcriptome analysis, are reconfirmed by independent qRT-PCR analysis. Three independent experiments were performed. Data represent mean  $\pm$  s.d. (E) JC-1 staining assays. Mitochondria with low membrane potential are in green and mitochondria with high membrane potential in red. (F) Relative Red/Green ratio was quantified by ImageJ. Data represent mean  $\pm$  s.d. of the 3 independent experiments. \*\*,  $P \leq 0.01$ . The Student *t* test was applied. (G) qRT-PCR analysis of *ppargc1a* in *nr1d1* mutants under DD condition. The mRNA expression pattern was analysis by JTK-CYCLE method. ADJ.P for adjusted minimal *P*-values (\*,  $P \leq 0.05$ ), AMP for amplitude. Two-way ANOVA with the Tukey *post hoc* test was conducted (\*\*\*,  $P \leq 0.001$ ). (H) A model for circadian regulation of autophagy in zebrafish. Transcription factor *cebpb* is regulated by the Clock-Arntl/Bmal1 heterodimer and induces autophagy rhythms in zebrafish and mice, while Nr1d1 directly controls autophagy genes through RORE. Further, nutritional signals can affect both autophagy and circadian rhythms in zebrafish.

coordinate to regulate autophagy rhythms needs to be investigated in the future, these 2 circadian regulatory mechanisms unambiguously play important roles in generation and maintenance of autophagy rhythms in zebrafish (Fig. 8G).

### **Nr1d1 is essential for the zebrafish circadian clock**

We found that under LD condition, *nr1d1* mutant fish display hyperactivity, similar to the phenotypes of zebrafish *per1b* null mutant but completely different from the zebrafish *per2* mutant (Figs. 3A, 3B and 3E).<sup>30,32</sup> Under DD conditions, *nr1d1* mutant fish show half-an-hour phase delay and 0.25-h shortened period, the *per1b* mutant fish show 2-h phase advance and half-hour shortened period,<sup>30</sup> and *per2* mutant fish show 2-h phase delay and 1.5-h lengthened period.<sup>32</sup> However, *nr1d1* knockout mice also display a 0.5-h shortened period under DD condition and mania-like behaviors.<sup>43</sup> Thus, Nr1d1 plays a conserved but distinct role in maintaining zebrafish locomotor rhythms.

We also found that *arntl/bmal* genes are significantly upregulated in *nr1d1* mutant fish, suggesting a key regulatory role of Nr1d1 in *arntl/bmal* transcription, consistent with previous results (Fig. 3G).<sup>32,55</sup> Both *cry1aa* and *cry1ab* are downregulated in *nr1d1* mutant zebrafish larvae (Fig. 3G), which is at odds with a previous report of upregulation of *Cry1* and *Cry2* in the *nr1d1* knockout mouse liver,<sup>55</sup> suggesting different roles of Nr1d1 in regulating *Cry* genes in zebrafish and mice. Further, we found that in the zebrafish liver, fasting upregulates *arntl1b/bmal1b* and *clocka/clock1a*, while *per1b*, *cry1ab* and *nr1d1* are phase-shifted (Fig. 7A). Thus, the disrupted locomotor rhythms and the altered expression of circadian clock genes we observed in the *nr1d1* mutant fish indicate that Nr1d1 is an indispensable component in the zebrafish circadian clock.

### **Extensive roles of Nr1d1 by transcriptome analysis**

Previous studies have revealed multiple functions of NR1D1 in mice.<sup>22,43,56,57</sup> Here, our transcriptome analysis shows that DEGs of *nr1d1* mutant zebrafish are involved in numerous life processes including autophagy, stress response, metabolism, and signal transduction (Figs. S4, S5 and Table S3). For instance, *atg10* (*autophagy-related 10 homolog*) and *exoc3* (*exocyst complex component 3*) (Fig. 8D), involved in autophagy signaling pathway or endoplasmic reticulum stress-induced autophagy,<sup>58</sup> are significantly upregulated in *nr1d1* mutant fish. For stress response, we observed significant upregulation of DNA repair genes including 6-4 photolyase, *ddb2* (*damage-specific DNA binding protein 2*) and *rbp4* (*retinol binding protein 4, plasma*) (Fig. 8D and Table S3), and heat shock gene *serpinb1* (*serine protease inhibitor, clade b (ovalbumin), member 1*), implicating the pathway for DNA repair of UV-induced damages or entrainment of the circadian clock by temperature are both disrupted in the *nr1d1* mutant fish.<sup>59-64</sup> A large number of DEGs such as *ucp3* (*uncoupling protein 3*), *gsk3b* (*glycogen synthase kinase 3 β*), *urod* (*uroporphyrinogen decarboxylase*), *cyp27a7* (*cytochrome P450, family 27, subfamily A, polypeptide 7*), and *gbgt1l4* (*globoside α-1,3-N-acetylgalactosaminyltransferase 1, like 4*) (Fig. 8D and Table S3), involved in thermogenic, energy metabolism, heme synthesis, oxidoreductase activity and immune response, are all altered, implicating metabolic

roles of Nr1d1 in zebrafish.<sup>20,56,65-67</sup> Further, as mitochondrial activities are intimately related with autophagy activities,<sup>54</sup> low mitochondrial activities and contents as revealed by JC-1 staining, and downregulation of *ppargc1a* expression in *nr1d1* mutant fish (Fig. 8E, 8F and 8G), suggesting that Nr1d1 is essential for maintaining zebrafish autophagy rhythms and altered autophagy activities in *nr1d1* mutant in turn results in off-balance of the cellular mitochondrial energy.<sup>22</sup> In addition, *gria3a* (*glutamate receptor, ionotropic, AMPA 3a*), *slc5a1* (*solute carrier family 5 (sodium/glucose cotransporter), member 1*), *fn1b* (*fibronectin 1b*) and *wdr3* (*WD repeat domain 3*), involved in signal transduction or cellular functions, also are disrupted in *nr1d1* mutant zebrafish (Fig. 8D and Table S3).<sup>68-70</sup> Even though the exact mechanisms underlying how *nr1d1* regulates these genes need detailed investigation in the future, our transcriptome analysis reveals that in addition to circadian and autophagy functions, zebrafish Nr1d1 contributes extensively to numerous life processes, setting the stage for investigation of its novel functions in the future.

In summary, our study provides, for the first time, clear evidence of how the circadian clock regulates autophagy rhythms, i.e., both E-box-mediated and RORE-mediated transcriptional regulatory mechanisms underlie circadian regulation of autophagy rhythms. Expression of autophagy genes and proteins and the number of mature autolysosomes are all upregulated without rhythmicity in *per1b* and TALEN-generated *nr1d1* mutant fish, suggesting *Per1b* and Nr1d1 are critical for maintaining autophagy rhythms. Disruption of expression of core circadian clock genes and circadian behaviors in *nr1d1* mutant indicates that Nr1d1 is also essential for the zebrafish circadian clock. Fasting results in altered expression of both circadian clock genes and autophagy genes in zebrafish adult peripheral organs. Further, transcriptome analysis implicates extensive roles of Nr1d1 in numerous life processes. Because altered autophagy changes normal triglyceride hydrolysis in lipid droplets and causes lipid metabolism disorders,<sup>1</sup> our study implicates that dysregulated autophagy derived from circadian misalignment or mutations of circadian clock genes such as *nr1d1* likely contributes to common metabolic diseases such as obesity.

## **Materials and methods**

### **Animals**

Wild-type AB strain zebrafish (*Danio rerio*), *nr1d1*, *per1b* mutant zebrafish were maintained on a 14 h/10 h light/dark cycle at the Soochow University Zebrafish Facility according to standard protocols. Embryos were collected from group crosses of 2 males and 2 females. All animal protocols were approved by the Soochow University Animal Ethics and Use Committee.

### **TALEN construction, mRNA synthesis and microinjection**

The right and left arms of TALEN targeting *nr1d1* were designed using a web-tool 'TALEN-NT',<sup>40</sup> and constructed using the 'unit assembly' method with Sharkey-AS and Sharkey-R forms of FokI cleavage domains as described previously.<sup>41</sup> Capped mRNAs of the TALEN expression vectors

were in vitro transcribed with Sp6 mMACHINE Kit (Thermo Fisher, AM1340), and microinjected in pair into one-cell zebrafish embryos at a concentration of 250 pg.

### **Mutagenesis frequencies and identification of *nr1d1* mutants**

The microinjected embryos were maintained in E3 medium (5 mM NaCl, 0.17 mM KCl, 0.33 mM CaCl<sub>2</sub>, 0.33 mM MgSO<sub>4</sub>) at 28.5°C. The survival rate of injected embryos was recorded at 1 d post fertilization (Table S2). Genomic DNAs were extracted from approximately 10 embryos at 2 dpf. A 426-bp DNA fragment containing the *nr1d1* target fragment was amplified by PCR (Primers used are listed in Table S1), and digested using BslI (NcoI). Estimated mutagenesis frequencies were calculated by software ImageJ as described previously.<sup>71</sup> The uncleaved bands were cloned into pMD 19T vector (Takara, D102C) for sequencing analysis. To identify the germ-line-transmitted mutations, the injected founder embryos were raised to adulthood and then outcrossed with wild types. Genomic DNAs were extracted from 8 F<sub>1</sub> embryos each cross, and analyzed via PCR amplification and sequencing as described above. Siblings of the F<sub>1</sub> embryos that carry heritable mutations were raised to adulthood and individual F<sub>1</sub> fish was reidentified via PCR amplification and sequencing with fin-clipped DNAs. Two *nr1d1*-null mutation lines were established.

### **Behavioral analysis for zebrafish**

Locomotor activity analysis was performed as described previously with modifications.<sup>72</sup> After the fourth d postfertilization, zebrafish larvae were placed into each well of 96-well plate singly. Locomotor activities of larvae were monitored and recorded for 4 consecutive d (14 h light and 10 h dark for LD or 24 h dark for DD) using an automate video-tracking system (Noldus, DanioVision, Wageningen, Netherlands). Locomotor activities were recorded from d 5 to d 8 postfertilization as the total distance moved by one larva during 10-min time duration. Data are presented as a moving average distance for each group (N = 48). The period length of each larval locomotor trace was retrieved. Statistical analysis of period length differences between the treatment groups was performed with one-way analysis of variance (ANOVA) followed by the Dunnett post-hoc test comparing each sample group with the control group.

### **RNA extraction and quantitative real-time PCR**

Total RNAs were extracted from approximately 50 larvae of homozygous *nr1d1* mutants or wild types at 4-h intervals from 72 to 96 h postfertilization (hpf) under LD or 96 to 120 hpf under DD, and adult organs (brain, liver, heart, eyes and testis, at least 5 fish for each sample) under the LD using TriZol (Invitrogen, 15596018). Quantitative real-time PCR (Thermo Fisher, StepOnePlus, 437660, Waltham, USA) was performed in ABI thermal profiles with the SYBR green detection system (Takara, RR420A) and a thermal profile of 40 cycles of 95°C, 10 s, 60°C, 30 s. Data represent mean ± s.d. of the 3 independent experiments. All primers used were listed in Table S1.

### **DNA site-directed mutagenesis and vector constructs**

Mutagenized DNA vectors were constructed by PCR-based site-directed mutagenesis. PCR was performed with KOD plus DNA polymerase (TOYOBO, KOD-201). A DpnI (NEB, R0176) restriction enzyme-treated PCR product was transformed into *E. coli*. Positive clones were randomly selected and verified by sequencing. A 2,000-bp fragment of the zebrafish *ulk1a* promoter region containing 2 RORE motifs and one Rev-DR2 motif was isolated and cloned into the luciferase reporter containing pGL 4.17 vector (Promega, 9PIE672), cloned into pcDNA 3.1 vector (Invitrogen, V790-20) or the pcDNA 3.1-FLAG vector (Addgene, 20011; deposited by Stephen Smale). All DNA constructs were confirmed by DNA sequencing. The primers used are listed in Table S1.

### **Protein extraction and western blotting**

Total proteins of zebrafish embryos were extracted with the tissue lysis buffer (50 mM Tris, pH 8.0, 150 mM NaCl, 2 mM EDTA, 1% NP-40, Thermo Fisher, 28324) and protein inhibitors (Roche, 04693116001) and then separated in 12% sodium dodecyl sulfate-PAGE gel. Western blotting was performed following the CST (Cell Signaling Technology) western blotting instruction. Protein bands were then transferred to a nitrocellulose member and incubated with desired antibodies as follows: Anti-mouse LC3B antibody (Cell Signaling Technology, 4108), SQSTM1/p62 (Cell Signaling Technology, 5114), anti-zebrafish Tuba1 antibody (Cell Signaling Technology, 2148) at a dilution of 1:1, 000 and then blocking with secondary antibodies at a dilution of 1:3, 000. Chemiluminescence Detection Kit (Biological Industries, 20-500-120) visualized the membranes. Tuba1 was used as a loading control. Data represent mean ± s.d. of the 3 independent studies.

### **Transmission electron microscopy (TEM)**

Zebrafish liver samples were fixed in 2.5 % glutaraldehyde buffer and embedded for 24 h, and their TEM images were acquired with a transmission electron microscope (Hitachi, H-600, Tokyo, Japan) at the Soochow University Electron Microscopy Core Facility. Autophagosome and autolysosome numbers were counted manually, and the cytoplasmic areas were quantified with software ImageJ.

### **JC-1 staining**

JC-1 mitochondrial membrane potential dye (MesGen Biotechnology, MG9621) was dissolved in DMSO to the concentration of 200 μM. Zebrafish larvae at 56 hpf were incubated with 10 μM of JC-1 dye at 37°C for 30 min. Three independent treatments were conducted. The JC-1 dye-stained larvae were photographed with a microscope (Olympus confocal microscope system, FV1200, Tokyo, Japan).

### **Cell transfection and luciferase reporter assay**

A 2,129-bp zebrafish *cebpb* promoter fragment or a 1,999-bp zebrafish *ulk1a* promoter fragment was PCR amplified and cloned into

pGL4.17 vector (Promega, 9PIE672), respectively. Human embryonic kidney (HEK) 293T cells were cultured in DMEM containing 10% serum and penicillin-streptomycin in a 24-well plate. Transfection was done with Lipofectamine 2000 (Invitrogen, 11668027) according to the manufacturer's instructions. Luciferase reporter assays were performed with a Dual-Report assay system (Promega, E1980). 100 ng each of *cebpb-luc*, *ulk1a-luc*, *clocka/clock1a*, *arntl1b/bmal1b* and *cry1ab* were used; for the dosage-dependent experiment, 100, 200 and 300 ng of *nr1d1* or *rora*, were used. The total DNA amounts were equalized by pcDNA 3.1 vector. Three independent experiments were conducted for each assay.

### Chromatin immunoprecipitation (ChIP) assays

ChIP assays were performed with Chromatin Immunoprecipitation Assay Kit (Millipore, 17-295). For the Arntl1b ChIP assay, the larvae were collected at 120 hpf and 132 hpf; for the FLAG-Nr1d1 ChIP assay, the microinjected larvae were collected at 72 hpf and 84 hpf. The larval samples were cross-linked in 2% formaldehyde for 10 min, and then fractionated with protein A Agarose (EMDmillipore, 16-157). Chromatin lysates were immunoprecipitated with Arntl1b antibodies (Abgent, customized, peptide PSSQLTQSPESDR) or negative control mouse IgG (Invitrogen, 10400C) in the presence of protein A Agarose-salmon sperm DNA (50% Slurry, EMDmillipore, 16-157).<sup>30</sup> Then DNA was purified using a purification kit (OMEGA, D2500) and subsequently analyzed by qRT-PCR using primers flanking the predicted binding sites in the promoter regions. Primers used for the ChIP assay are listed in Table S1.

### Pharmacological treatment

GSK4112 (Sigma, G0673) were dissolved in DMSO at concentrations of 100  $\mu$ M or 50  $\mu$ M, respectively. Zebrafish larvae at 72 hpf and 84 hpf were incubated in 20  $\mu$ M of GSK4112 for 24 h at 28.5°C, respectively. Three independent treatments for each drug were performed.

### Restricting feeding experiment

Four-month-old wild-type and *nr1d1* mutant zebrafish were starved for 2 consecutive wk for the restricting feeding experiment as previously described.<sup>73</sup> The brains, the livers, the hearts, the eyes, and the intestines of at least 5 males each from the *nr1d1* mutant, fasted *nr1d1* mutant, fasted wild-type and wild-type fish were then dissected out at 12 time points with 4-h interval for 2 consecutive days for RNA extraction and qRT-PCR analysis. At least 3 independent experiments were done for each time point under examination.

### Deep sequencing-based transcriptome analysis of *nr1d1* mutant fish

1. *RNA quantification and qualification.* Total RNAs from 2 stages, 122 hpf (CT2) and 134 hpf (CT14) were used. RNAs were examined on 1% agarose gels, purity and concentrations was checked with a Nanodrop 2000 spectrophotometer (Thermo Fisher, Waltham, USA). 2. *Library preparation for sequencing.* A total amount of 3  $\mu$ g RNA per sample was used

for the RNA sample preparations. Sequencing libraries were generated using NEBNext→Ultra™ RNA Library Prep Kit (NEB, USA) following the manufacturer's instructions. 3. *Clustering and sequencing.* Clustering of the index-coded samples was performed on a cBot Cluster Generation System using TruSeq PE Cluster Kit (Illumina, PE-401-3001) according to the manufacturer's instructions. After clustering, the library preparations were sequenced on an Illumina HiSeq 2000 platform. 4. *Quality control.* We used Perl scripts for removing the adapter for clean reads, calculated the Q20, Q30, GC-content, duplication data and then generated the Raw reads. All the following analyses were based on clean data with high quality. 5. *Transcriptome assembly.* Transcriptome assembly was performed according to the protocol described previously.<sup>74</sup> 6. *Gene functional annotation.* For the Gene Ontology (GO) enrichment analysis, the differentially expressed genes (DEGs) was implemented by the Goseq R packages based Wallonia noncentral hyper-geometric distribution;<sup>75</sup> For the Kyoto Encyclopedia of Genes and Genomes (KEGG) analysis, we used KOBAS software to test the statistical enrichment of DEGs in KEGG pathways to predict and classify functions of the assembled sequences (Mao et al, 2005).<sup>76</sup> 7. *Quantification of gene expression levels.* Gene expression levels were estimated by RSEM for each RNA sample.<sup>77</sup>

### Heatmaps

For the behavior assays, heatmaps were constructed by an automated video-tracking system software EthoVision XT10 (Noldus, DanioVision, Wageningen, Netherlands). For the ADJ.P values and correlation efficiencies in different organs of wild-type-fed, wild-type fasted, *nr1d1*-fed and *nr1d1* fasted, heatmaps were made with custom scripts and implemented in R.

### Statistical analysis

Values are means  $\pm$  s.d. of the indicated number of measurements. Statistical significance was determined using the 2-tailed unpaired Student *t* test or one-way ANOVA or 2-way ANOVA with a significance of  $P \leq 0.05$ . In particular, multivariate experiments (e.g., time points and mutants) were analyzed using 2-way ANOVA with the Tukey *post hoc* test. A repeated-measure adjustment was employed when appropriate (e.g., daily onset profiles). An *F* test was used to assess the differences in variability to circadian-mutant shifts or time points between genotypes. For the JTK-CYCLE analysis, each parameter was recorded and analyzed as previously described by R<sup>2</sup>. All statistical analyses were performed using SPSS 16.0 software.

### Abbreviations

<i>atg4a</i>	autophagy-related 4 homolog A
<i>atp6v1d</i>	ATPase H <sup>+</sup> transporting V1 subunit D
<i>becn1/beclin1</i>	myosin-like BCL2 interacting protein
<i>bnip3</i>	BCL2/adenovirus E1B interacting protein 3
<i>arntl/bmal</i>	brain and muscle aryl hydrocarbon receptor nuclear translocator (ARNT)-like
CCGs	circadian controlled genes

clock	clock circadian regulator
ChIP	chromatin immunoprecipitation
cry	cryptochrome circadian clock
DD	dark/dark
DEGs	differentially expressed genes
gabarapa	GABA(A) receptor-associated protein a
gsk4112	agonist of nr1d1
period	period circadian clock
LD	light/dark
Map1lc3b	microtubule-associated protein 1 light chain 3 $\beta$
RT-PCR	reverse transcriptase-polymerase chain reaction
ppargc1a/pgc1a	peroxisome proliferator-activated receptor gamma, coactivator 1 $\alpha$
Sqstm1/p62	sequestosome 1
TALEN	transcription activator-like effector nucleases
TEM	transmission electron microscopy
Ulk1	unc-51 like autophagy activating kinase 1

## Disclosure of potential conflicts of interest

No potential conflicts of interest were disclosed.

## Acknowledgments

We wish to thank Bo Zhang from Peking University for providing TALEN Unit Assembly vectors, Weijun Pan from Shanghai Institutes for Biological Sciences, the Chinese Academy of Sciences for providing the mCherry-map1lc3b plasmid, Yilin Yan from the University of Oregon and Yingbin Zhong of our lab for discussion and critical reading of the manuscript, and Zhaomin Zhong for maintaining fish lines and assistance in behavioral assays.

## Funding

This work was supported by the grants from National Basic Research Program of China (973 Program) (2012CB947600), the National Natural Science Foundation of China (NSFC) (31030062), National High Technology Research and Development Program of China (863 Program) (2011AA100402-2), the Jiangsu Distinguished Professorship Program (SR13400111), and the Natural Science Foundation of Jiangsu Province (BK2012052), the Priority Academic Program Development (PAPD) of Jiangsu Higher Education Institutions (YX13400214), the High-Level Innovative Team of Jiangsu Province, and the “333” project of Jiangsu Province (BRA2015328).

## References

- Walther TC, Farese RV, Jr. Lipid droplets and cellular lipid metabolism. *Ann Rev Biochem* 2012; 81:687-714; PMID:22524315; <http://dx.doi.org/10.1146/annurev-biochem-061009-102430>
- Hughes ME, Hogenesch JB, Kornacker K. JTK\_CYCLE: an efficient nonparametric algorithm for detecting rhythmic components in genome-scale data sets. *J Biol Rhythms* 2010; 25:372-80; PMID:20876817; <http://dx.doi.org/10.1177/0748730410379711>
- Panda S, Hogenesch JB, Kay SA. Circadian rhythms from flies to human. *Nature* 2002; 417:329-35; PMID:12015613; <http://dx.doi.org/10.1038/417329a>
- Ueda HR, Chen W, Adachi A, Wakamatsu H, Hayashi S, Takasugi T, Nagano M, Nakahama K, Suzuki Y, Sugano S, et al. A transcription factor response element for gene expression during circadian night. *Nature* 2002; 418:534-9; PMID:12152080; <http://dx.doi.org/10.1038/nature00906>
- Ko CH, Takahashi JS. Molecular components of the mammalian circadian clock. *Hum Mol Genetics* 2006; 15 Spec No 2:R271-7; <http://dx.doi.org/10.1093/hmg/ddl207>
- Cho H, Zhao X, Hatori M, Yu RT, Barish GD, Lam MT, Chong LW, DiTacchio L, Atkins AR, Glass CK, et al. Regulation of circadian behaviour and metabolism by REV-ERB- $\alpha$  and REV-ERB- $\beta$ . *Nature* 2012; 485:123-7; PMID:22460952; <http://dx.doi.org/10.1038/nature11048>
- Kumaki Y, Ukai-Tadenuma M, Uno KD, Nishio J, Masumoto KH, Nagano M, Komori T, Shige-yoshi Y, Hogenesch JB, Ueda HR, et al. Analysis and synthesis of high-amplitude Cis-elements in the mammalian circadian clock. *Proc Natl Acad Sci U S A* 2008; 105:14946-51; PMID:18815372; <http://dx.doi.org/10.1073/pnas.0802636105>
- Mizushima N, Levine B, Cuervo AM, Klionsky DJ. Autophagy fights disease through cellular self-digestion. *Nature* 2008; 451:1069-75; PMID:18305538; <http://dx.doi.org/10.1038/nature06639>
- Rabinowitz JD, White E. Autophagy and metabolism. *Science* 2010; 330:1344-8; PMID:21127245; <http://dx.doi.org/10.1126/science.1193497>
- Wong PM, Puente C, Ganley IG, Jiang X. The ULK1 complex: sensing nutrient signals for autophagy activation. *Autophagy* 2013; 9:124-37; PMID:23295650; <http://dx.doi.org/10.4161/auto.23323>
- Ganley IG, Lam du H, Wang J, Ding X, Chen S, Jiang X. ULK1, ATG13, FIP200 complex mediates mTOR signaling and is essential for autophagy. *J Biol Chem* 2009; 284:12297-305; PMID:19258318; <http://dx.doi.org/10.1074/jbc.M900573200>
- Kuma A, Mizushima N. Physiological role of autophagy as an intracellular recycling system: with an emphasis on nutrient metabolism. *Seminars Cell Dev Biol* 2010; 21:683-90; <http://dx.doi.org/10.1016/j.semdb.2010.03.002>
- Liang XH, Jackson S, Seaman M, Brown K, Kempkes B, Hibshoosh H, Levine B. Induction of autophagy and inhibition of tumorigenesis by beclin 1. *Nature* 1999; 402:672-6; PMID:10604474; <http://dx.doi.org/10.1038/45257>
- Pfeifer U, Scheller H. A morphometric study of cellular autophagy including diurnal variations in kidney tubules of normal rats. *J Cell Biol* 1975; 64:608-21; PMID:1171105; <http://dx.doi.org/10.1083/jcb.64.3.608>
- Reme CE, Sulser M. Diurnal variation of autophagy in rod visual cells in the rat. *Albrecht Von Graefes Archiv Klin Exp Ophthalmol* 1977; 203:261-70; PMID:303474; <http://dx.doi.org/10.1007/BF00409832>
- Ma D, Panda S, Lin JD. Temporal orchestration of circadian autophagy rhythm by C/EBPbeta. *EMBO J* 2011; 30:4642-51; PMID:21897364; <http://dx.doi.org/10.1038/emboj.2011.322>
- Duez H, van der Veen JN, Duhem C, Pourcet B, Touvier T, Fontaine C, Derudas B, Baugé E, Havinga R, Bloks VW, et al. Regulation of bile acid synthesis by the nuclear receptor Rev-erbalpha. *Gastroenterol* 2008; 135:689-98; <http://dx.doi.org/10.1053/j.gastro.2008.05.035>
- Fontaine C, Dubois G, Duguay Y, Helledie T, Vu-Dac N, Gervois P, Soncin F, Mandrup S, Fruchart JC, Fruchart-Najib J, et al. The orphan nuclear receptor Rev-Erbalpha is a peroxisome proliferator-activated receptor (PPAR) gamma target gene and promotes PPAR-gamma-induced adipocyte differentiation. *J Biol Chem* 2003; 278:37672-80; PMID:12821652; <http://dx.doi.org/10.1074/jbc.M304664200>
- Fontaine C, Rigamonti E, Pourcet B, Duez H, Duhem C, Fruchart JC, Chinetti-Gbaguidi G, Staels B. The nuclear receptor Rev-erbalpha is a liver X receptor (LXR) target gene driving a negative feedback loop on select LXR-induced pathways in human macrophages. *Mol Endocrinol* 2008; 22:1797-811; PMID:18511497; <http://dx.doi.org/10.1210/me.2007-0439>
- Yin L, Wu N, Curtin JC, Qatanani M, Szwegold NR, Reid RA, Waitt GM, Parks DJ, Pearce KH, Wisely GB, et al. Rev-erbalpha, a heme sensor that coordinates metabolic and circadian pathways. *Sci* 2007; 318:1786-9; <http://dx.doi.org/10.1126/science.1150179>
- Raghuram S, Stayrook KR, Huang P, Rogers PM, Nosie AK, McClure DB, Burris LL, Khorasanizadeh S, Burris TP, Rastinejad F. Identification of heme as the ligand for the orphan nuclear receptors REV-ERBalpha and REV-ERBbeta. *Nat Structural Mol Biol* 2007; 14:1207-13; <http://dx.doi.org/10.1038/nsmb1344>



- [22] Woldt E, Sebti Y, Solt LA, Duhem C, Lancel S, Eeckhoutte J, Hesselink MK, Paquet C, Delhaye S, Shin Y, et al. Rev-erb- $\alpha$  modulates skeletal muscle oxidative capacity by regulating mitochondrial biogenesis and autophagy. *Nat Med* 2013; 19:1039-46; PMID:23852339; <http://dx.doi.org/10.1038/nm.3213>
- [23] He C, Klionsky DJ. Analyzing autophagy in zebrafish. *Autophagy* 2010; 6:642-4; PMID:20495344; <http://dx.doi.org/10.4161/auto.6.5.12092>
- [24] He C, Bartholomew CR, Zhou W, Klionsky DJ. Assaying autophagic activity in transgenic GFP-Lc3 and GFP-Gabarap zebrafish embryos. *Autophagy* 2009; 5:520-6; PMID:19221467; <http://dx.doi.org/10.4161/auto.5.4.7768>
- [25] Appelbaum L, Wang GX, Maro GS, Mori R, Tovin A, Marin W, Yokogawa T, Kawakami K, Smith SJ, Gothilf Y, et al. Sleep-wake regulation and hypocretin-melatonin interaction in zebrafish. *Proc Natl Acad Sci U S A* 2009; 106:21942-7; PMID:19966231; <http://dx.doi.org/10.1073/pnas.906637106>
- [26] Huang P, Xiao A, Zhou M, Zhu Z, Lin S, Zhang B. Heritable gene targeting in zebrafish using customized TALENs. *Nat Biotechnol* 2011; 29:699-700; PMID:2182242; <http://dx.doi.org/10.1038/nbt.1939>
- [27] Wang D, Jao LE, Zheng N, Dolan K, Ivey J, Zonies S, Wu X, Wu K, Yang H, Meng Q, et al. Efficient genome-wide mutagenesis of zebrafish genes by retroviral insertions. *Proc Natl Acad Sci U S A* 2007; 104:12428-33; PMID:17640903; <http://dx.doi.org/10.1073/pnas.0705502104>
- [28] Wienholds E, van Eeden F, Kusters M, Mudde J, Plasterk RH, Cuppen E. Efficient target-selected mutagenesis in zebrafish. *Genome Res* 2003; 13:2700-7; PMID:14613981; <http://dx.doi.org/10.1101/gr.1725103>
- [29] Hwang WY, Fu Y, Reyon D, Maeder ML, Tsai SQ, Sander JD, Peterson RT, Yeh JR, Joung JK. Efficient genome editing in zebrafish using a CRISPR-Cas system. *Nat Biotechnol* 2013; 31:227-9; PMID:23360964; <http://dx.doi.org/10.1038/nbt.2501>
- [30] Huang J, Zhong Z, Wang M, Chen X, Tan Y, Zhang S, He W, He X, Huang G, Lu H, et al. Circadian modulation of dopamine levels and dopaminergic neuron development contributes to attention deficiency and hyperactive behavior. *J Neurosci* 2015; 35:2572-87; PMID:25673850; <http://dx.doi.org/10.1523/JNEUROSCI.2551-14.2015>
- [31] Tan Y, DeBruyne J, Cahill GM, Wells DE. Identification of a mutation in the Clock1 gene affecting zebrafish circadian rhythms. *J Neurogenetics* 2008; 22:149-66; <http://dx.doi.org/10.1080/01677060802049738>
- [32] Wang M, Zhong Z, Zhong Y, Zhang W, Wang H. The Zebrafish period2 protein positively regulates the circadian clock through mediation of retinoic acid receptor (RAR)-related orphan receptor  $\alpha$  (Roralpha). *J Biol Chem* 2015; 290:4367-82; PMID:25544291; <http://dx.doi.org/10.1074/jbc.M114.605022>
- [33] Kyostila K, Syrja P, Jagannathan V, Chandrasekar G, Jokinen TS, Seppala EH, Becker D, Drögemüller M, Dietschi E, Drögemüller C, et al. A missense change in the ATG4D gene links aberrant autophagy to a neurodegenerative vacuolar storage disease. *PLoS Genetics* 2015; 11:e1005169; PMID:25875846; <http://dx.doi.org/10.1371/journal.pgen.1005169>
- [34] Eskelinen EL. To be or not to be? Examples of incorrect identification of autophagic compartments in conventional transmission electron microscopy of mammalian cells. *Autophagy* 2008; 4:257-60; PMID:17986849; <http://dx.doi.org/>; <http://dx.doi.org/10.4161/auto.5179>
- [35] Delaunay F, Thisse C, Marchand O, Laudet V, Thisse B. An inherited functional circadian clock in zebrafish embryos. *Science* 2000; 289:297-300; PMID:10894777; <http://dx.doi.org/10.1126/science.289.5477.297>
- [36] Cretenet G, Le Clech M, Gachon F. Circadian clock-coordinated 12 Hr period rhythmic activation of the IRE1alpha pathway controls lipid metabolism in mouse liver. *Cell Metab* 2010; 11:47-57; PMID:20074527; <http://dx.doi.org/10.1016/j.cmet.2009.11.002>
- [37] He C, Klionsky DJ. Regulation mechanisms and signaling pathways of autophagy. *Ann Rev Genet* 2009; 43:67-93; <http://dx.doi.org/10.1146/annurev-genet-102808-114910>
- [38] Moscat J, Diaz-Meco MT. p62 at the crossroads of autophagy, apoptosis, and cancer. *Cell* 2009; 137:1001-4; PMID:19524504; <http://dx.doi.org/10.1016/j.cell.2009.05.023>
- [39] Lattante S, de Calbiac H, Le Ber I, Brice A, Ciura S, Kabashi E. Sqstm1 knock-down causes a locomotor phenotype ameliorated by rapamycin in a zebrafish model of ALS/FTLD. *Hum Mol Genetics* 2015; 24:1682-90; <http://dx.doi.org/10.1093/hmg/ddu580>
- [40] Doyle EL, Booher NJ, Standage DS, Voytas DF, Brendel VP, Vandyk JK, Bogdanove AJ. TAL Effector-Nucleotide Targeter (TALE-NT) 2.0: tools for TAL effector design and target prediction. *Nucleic Acids Res* 2012; 40:W117-22; PMID:22693217; <http://dx.doi.org/10.1093/nar/gks608>
- [41] Huang P, Xiao A, Tong X, Zu Y, Wang Z, Zhang B. TALEN construction via "Unit Assembly" method and targeted genome modifications in zebrafish. *Methods* 2014; 69:67-75; PMID:24556555; <http://dx.doi.org/10.1016/j.ymeth.2014.02.010>
- [42] del Pozo A, Sanchez-Ferez JA, Sanchez-Vazquez FJ. Circadian rhythms of self-feeding and locomotor activity in zebrafish (Danio Rerio). *Chronobiol Int* 2011; 28:39-47; PMID:21182403; <http://dx.doi.org/10.3109/07420528.2010.530728>
- [43] Chung S, Lee EJ, Yun S, Choe HK, Park SB, Son HJ, Kim KS, Dluzen DE, Lee I, Hwang O, et al. Impact of circadian nuclear receptor REV-ERBalpha on midbrain dopamine production and mood regulation. *Cell* 2014; 157:858-68; PMID:24813609; <http://dx.doi.org/10.1016/j.cell.2014.03.039>
- [44] Sasaki T, Lian S, Qi J, Bayliss PE, Carr CE, Johnson JL, Guha S, Kobler P, Catz SD, Gill M, et al. Aberrant autolysosomal regulation is linked to the induction of embryonic senescence: differential roles of Beclin 1 and p53 in vertebrate Spns1 deficiency. *PLoS Genetics* 2014; 10:e1004409; PMID:24967584; <http://dx.doi.org/10.1371/journal.pgen.1004409>
- [45] Yang Z, Klionsky DJ. An overview of the molecular mechanism of autophagy. *Curr Topics Microbiol Immunol* 2009; 335:1-32.
- [46] Xiong X, Tao R, DePinho RA, Dong XC. The autophagy-related gene 14 (Atg14) is regulated by forkhead box O transcription factors and circadian rhythms and plays a critical role in hepatic autophagy and lipid metabolism. *J Biol Chem* 2012; 287:39107-14; PMID:22992773; <http://dx.doi.org/10.1074/jbc.M112.412569>
- [47] Shigeyoshi Y, Taguchi K, Yamamoto S, Takekida S, Yan L, Tei H, Moriya T, Shibata S, Loros JJ, Dunlap JC, et al. Light-induced resetting of a mammalian circadian clock is associated with rapid induction of the mPer1 transcript. *Cell* 1997; 91:1043-53; PMID:9428526; [http://dx.doi.org/10.1016/S0092-8674\(00\)80494-8](http://dx.doi.org/10.1016/S0092-8674(00)80494-8)
- [48] Dekens MP, Whitmore D. Autonomous onset of the circadian clock in the zebrafish embryo. *EMBO J* 2008; 27:2757-65; PMID:18800057; <http://dx.doi.org/10.1038/emboj.2008.183>
- [49] Ukai H, Ueda HR. Systems biology of mammalian circadian clocks. *Ann Rev Physiol* 2010; 72:579-603; <http://dx.doi.org/10.1146/annurev-physiol-073109-130051>
- [50] Kakizawa T, Nishio S, Triqueneaux G, Bertrand S, Rambaud J, Laudet V. Two differentially active alternative promoters control the expression of the zebrafish orphan nuclear receptor gene Rev-erbalpha. *J Mol Endocrinol* 2007; 38:555-68; PMID:17496157; <http://dx.doi.org/10.1677/JME-06-0063>
- [51] Grant D, Yin L, Collins JL, Parks DJ, Orband-Miller LA, Wisely GB, Joshi S, Lazar MA, Willson TM, Zuercher WJ. GSK4112, a small molecule chemical probe for the cell biology of the nuclear heme receptor Rev-erbalpha. *ACS Chem Biol* 2010; 5:925-32; PMID:20677822; <http://dx.doi.org/10.1021/cb100141y>
- [52] Amaral IP, Johnston IA. Circadian expression of clock and putative clock-controlled genes in skeletal muscle of the zebrafish. *Am J Physiol Regulatory, Integrative Comparative Physiol* 2012; 302:R193-206; <http://dx.doi.org/10.1152/ajpregu.00367.2011>
- [53] Sanchez JA, Sanchez-Vazquez FJ. Feeding entrainment of daily rhythms of locomotor activity and clock gene expression in zebrafish brain. *Chronobiol Int* 2009; 26:1120-35; PMID:19731109; <http://dx.doi.org/10.3109/07420520903232092>
- [54] Mai S, Muster B, Bereiter-Hahn J, Jendrach M. Autophagy proteins LC3B, ATG5 and ATG12 participate in quality control after mitochondrial damage and influence lifespan. *Autophagy* 2012; 8:47-62; PMID:22170153; <http://dx.doi.org/10.4161/auto.8.1.18174>
- [55] Preitner N, Damiola F, Lopez-Molina L, Zakany J, Duboule D, Albrecht U, Schibler U. The orphan nuclear receptor REV-ERBalpha controls circadian transcription within the positive

- limb of the mammalian circadian oscillator. *Cell* 2002; 110:251-60; PMID:12150932; [http://dx.doi.org/10.1016/S0092-8674\(02\)00825-5](http://dx.doi.org/10.1016/S0092-8674(02)00825-5)
- [56] Gerhart-Hines Z, Feng D, Emmett MJ, Everett LJ, Loro E, Briggs ER, Bugge A, Hou C, Ferrara C, Seale P, et al. The nuclear receptor Rev-erbalpha controls circadian thermogenic plasticity. *Nature* 2013; 503:410-3; PMID:24162845; <http://dx.doi.org/10.1038/nature12642>
- [57] Zhang Y, Fang B, Emmett MJ, Damle M, Sun Z, Feng D, Armour SM, Reimsberg JR, Jager J, Soccio RE, et al. Discrete functions of nuclear receptor Rev-erbalpha couple metabolism to the clock. *Science* 2015; 348(6242):1488-92
- [58] Sakaki K, Yoshina S, Shen X, Han J, DeSantis MR, Xiong M, Mitani S, Kaufman RJ. RNA surveillance is required for endoplasmic reticulum homeostasis. *Proc Natl Acad Sci U S A* 2012; 109:8079-84; PMID:22562797; <http://dx.doi.org/10.1073/pnas.1110589109>
- [59] Selby CP, Sancar A. A cryptochrome/photolyase class of enzymes with single-stranded DNA-specific photolyase activity. *Proc Natl Acad Sci U S A* 2006; 103:17696-700; PMID:17062752; <http://dx.doi.org/10.1073/pnas.0607993103>
- [60] Guo C, Tang TS, Friedberg EC. SnapShot: nucleotide excision repair. *Cell* 2010; 140:754-4 e1; PMID:20211143; <http://dx.doi.org/10.1016/j.cell.2010.02.033>
- [61] Isken A, Golczak M, Oberhauser V, Hunzelmann S, Driever W, Imanishi Y, Palczewski K, von Lintig J. RBP4 disrupts vitamin A uptake homeostasis in a STRA6-deficient animal model for Matthew-Wood syndrome. *Cell Metab* 2008; 7:258-68; PMID:18316031; <http://dx.doi.org/10.1016/j.cmet.2008.01.009>
- [62] Ahn SG, Thiele DJ. Redox regulation of mammalian heat shock factor 1 is essential for Hsp gene activation and protection from stress. *Genes Dev* 2003; 17:516-28; PMID:12600944; <http://dx.doi.org/10.1101/gad.1044503>
- [63] Kornmann B, Schaad O, Bujard H, Takahashi JS, Schibler U. System-driven and oscillator-dependent circadian transcription in mice with a conditionally active liver clock. *PLoS Biol* 2007; 5:e34; PMID:17298173; <http://dx.doi.org/10.1371/journal.pbio.0050034>
- [64] Li W, Giles C, Li S. Insights into how Spt5 functions in transcription elongation and repressing transcription coupled DNA repair. *Nucleic Acids Res* 2014; 42:7069-83; PMID:24813444; <http://dx.doi.org/10.1093/nar/gku333>
- [65] Lam MT, Cho H, Lesch HP, Gosselin D, Heinz S, Tanaka-Oishi Y, Benner C, Kaikkonen MU, Kim AS, Kosaka M, et al. Rev-Erbs repress macrophage gene expression by inhibiting enhancer-directed transcription. *Nature* 2013; 498:511-5; PMID:23728303; <http://dx.doi.org/10.1038/nature12209>
- [66] Gibbs JE, Blaikley J, Beesley S, Matthews L, Simpson KD, Boyce SH, Farrow SN, Else KJ, Singh D, Ray DW, et al. The nuclear receptor REV-ERBalpha mediates circadian regulation of innate immunity through selective regulation of inflammatory cytokines. *Proc Natl Acad Sci USA* 2012; 109:582-7; PMID:22184247; <http://dx.doi.org/10.1073/pnas.1106750109>
- [67] Lee MS. Role of islet  $\beta$  cell autophagy in the pathogenesis of diabetes. *Trends Endocrinol Metabol* 2014; 25:620-7; <http://dx.doi.org/10.1016/j.tem.2014.08.005>
- [68] Wu Y, Arai AC, Rumbaugh G, Srivastava AK, Turner G, Hayashi T, Suzuki E, Jiang Y, Zhang L, Rodriguez J, et al. Mutations in ionotropic AMPA receptor 3 alter channel properties and are associated with moderate cognitive impairment in humans. *Proc Natl Acad Sci USA* 2007; 104:18163-8; PMID:17989220; <http://dx.doi.org/10.1073/pnas.0708699104>
- [69] Hoppmann V, Wu JJ, Soviknes AM, Helvik JV, Becker TS. Expression of the eight AMPA receptor subunit genes in the developing central nervous system and sensory organs of zebrafish. *Dev Dynamics* 2008; 237:788-99; <http://dx.doi.org/10.1002/dvdy.21447>
- [70] Cheng P, Andersen P, Hassel D, Kaynak BL, Limphong P, Juergensen L, Kwon C, Srivastava D. Fibronectin mediates mesendodermal cell fate decisions. *Development* 2013; 140:2587-96; PMID:23715551 <http://dx.doi.org/10.1242/dev.089052>
- [71] Reyon D, Tsai SQ, Khayter C, Foden JA, Sander JD, Joung JK. FLASH assembly of TALENs for high-throughput genome editing. *Nat Biotechnol* 2012; 30:460-5; PMID:22484455; <http://dx.doi.org/10.1038/nbt.2170>
- [72] Smadja Storz S, Tovin A, Mracek P, Alon S, Foulkes NS, Gothilf Y. Casein kinase 1delta activity: a key element in the zebrafish circadian timing system. *Plos One* 2013; 8:e54189; PMID:23349822; <http://dx.doi.org/10.1371/journal.pone.0054189>
- [73] Craig PM, Moon TW. Fasted zebrafish mimic genetic and physiological responses in mammals: a model for obesity and diabetes?. *Zebrafish* 2011; 8:109-17; PMID:21854210; <http://dx.doi.org/10.1089/zeb.2011.0702>
- [74] Grabherr MG, Haas BJ, Yassour M, Levin JZ, Thompson DA, Amit I, Adiconis X, Fan L, Raychowdhury R, Zeng Q, et al. Full-length transcriptome assembly from RNA-Seq data without a reference genome. *Nat Biotechnol* 2011; 29:644-52; PMID:21572440; <http://dx.doi.org/10.1038/nbt.1883>
- [75] Young MD, Wakefield MJ, Smyth GK, Oshlack A. Gene ontology analysis for RNA-seq: accounting for selection bias. *Genome Biol* 2010; 11:R14; PMID:20132535; <http://dx.doi.org/10.1186/gb-2010-11-2-r14>
- [76] Kanehisa M, Araki M, Goto S, Hattori M, Hirakawa M, Itoh M, Katayama T, Kawashima S, Okuda S, Tokimatsu T, et al. KEGG for linking genomes to life and the environment. *Nucleic Acids Res* 2008; 36:D480-4; PMID:18077471; <http://dx.doi.org/10.1093/nar/gkm882>
- [77] Li B, Dewey CN. RSEM: accurate transcript quantification from RNA-Seq data with or without a reference genome. *BMC Bioinformatics* 2011; 12:323; PMID:21816040; <http://dx.doi.org/10.1186/1471-2105-12-323>